The University of Alberta
Printing Department
Edmonton, Alberta

THE UNIVERSITY OF ALBERTA

AN OPTICAL TECHNIQUE FOR INVESTIGATING DIELECTRIC BREAKDOWN

by

© PATRICK J.C. RYALL

A THESIS

SUBMITTED TO THE FACULTY OF GRADUATE STUDIES

IN PARTIAL FULFILMENT OF THE REQUIREMENTS FOR THE DEGREE

OF MASTER OF SCIENCE

DEPARTMENT OF ELECTRICAL ENGINEERING

EDMONTON, ALBERTA

FALL, 1970

ABSTRACT

The surface deformation on a dielectric under static electric fields prior to and during breakdown was observed. A Fabry-Perot interferometer was used with one plate being the upper electrode and a titania disc surface acting as the reflecting plate. As the voltage was increased to breakdown, no surface movement was observed since the currents measured in this experiment were about two orders of magnitude less than those previously reported for similar experiments. After achieving a suitable coating on the upper plate, it was possible to observe the sequence of events during breakdown by recording the fringes with a high speed motion picture camera.

In the course of establishing the parameters for this experiment, measurements of the voltage distribution across the titania and vacuum gap were carried out and previous results essentially confirmed.

In the search for a suitable transparent conducting coating, various metal films and stannic oxide were investigated. The optical properties of Chromium films thinner than 100Å were established.

ACKNOWLEDGEMENT

The author gratefully acknowledges the encouragement and guidance received from the supervising professor, Dr. E. Sang throughout the course of this research.

The author wishes to express his appreciation to Mr. E. Buck and his staff for their help in the construction of the apparatus and especially to Mr. B. Arnold for his untiring work in the preparation of the optical flat.

The author also wishes to thank Mr. D. Sands for his help in filming the interference fringes.

The author is further indebted to the National Research Council and the University of Alberta for financial assistance.

TABLE OF CONTENTS

LIST OF ILLUSTRATIONS

PART I

MEASUREMENT OF VOLTAGE DISTRIBUTION ACROSS

TITANIA AND VACUUM GAP

1. INTRODUCTION

Titania has aroused considerable interest as a dielectric material because of its combination of a high dielectric constant. 95, and a low loss tangent, 0.0003. Many attempts to use these excellent properties have encountered considerable difficulties due to the breakdown of the titania at voltages lower than expected.

Work has been done in an effort to find the cause of this premature breakdown both in microwave windows and in dielectric-loaded slow-wave structures. A glaze consisting mainly of lead borate has been shown[1] to give an improvement in breakdown strength. Work has been done by R. Hayes[2] to obtain information about the breakdown process and to determine the properties of the glaze responsible for the improvement in breakdown strength. In work with static fields it was shown that for most dielectrics the breakdown strength is improved by spark conditioning phenomena but for titania permanent damage is caused at the onset of the sparking due to the reduction of the titania. The glaze prevents the sparking from damaging the surface.

Englefield et al.[4] and Toso[3] investigated the breakdown of titania and a vacuum gap in series. They showed that field emission causes a change in the amount of charge at the surface of the titania and hence a redistribution of voltage across the gap. The conclusions were reached on the basis of temperature, current and field emission readings and were further evidenced by mechanical measurements of

the force across the vacuum gap.

The intent of the present work is to investigate the voltage distribution as a function of vacuum gap spacing by electromechanical means and to observe any distortions of the surface as they occur. It has been suggested that before breakdown there may be some inhomogeneity in the electric field and that this would cause a distortion in the surface of the titania.

2. FORCE ACROSS THE VACUUM GAP

In order to be able to correlate the surface effects observed on the titania surface with the field strength across the vacuum gap, it was necessary to know the relation between the applied voltage and the voltage across the vacuum gap.

There has been strong evidence in previous work that the titania supports a much larger voltage than expected from theoretical considerations. When initially applied, most of the voltage exists across the vacuum gap due to the high dielectric constant of the titania. The high voltage changes the amount of charge present at the surface of the titania, causing cathode emission leading to a redistribution of voltage. In order to measure the magnitude of this effect, the voltage at the surface of the titania disc is calculated by measuring the mechanical force across the vacuum gap.

Two different cases were considered : 1) the case where the dielectric was attached to the positive electrode (ceramic anode) - referred to as a negative vacuum gap, 2) the case where the dielectric was attached to the negative electrode (ceramic cathode) - referred to as the positive vacuum gap. This terminology was used to remain consistent with previous work.

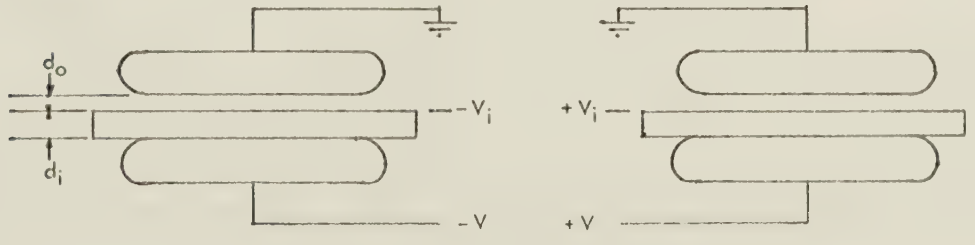

positive vacuum gap negative vacuum gap

figure 2.1

The force of attraction per unit area on the surface of a parallel plate capacitor is given by :

$$f = \sigma^2/2\varepsilon_o \qquad (2.1)$$

where f is force per unit area in Newtons $/m^2$, σ is surface charge density in Coulombs$/m^2$, and ε_o is the permittivity in $C/N.m^2$. Now the field in the capacitor is given by $E = \sigma/\varepsilon_o$, but E is also given by $E = V_i/d_o$, hence one may write :

$$f = \varepsilon_o V_i^2/(2d_o^2) \qquad (2.2)$$

where V_i, the voltage across the vacuum gap, equals aV, the applied voltage times 'a' the ratio between the two; d_o is the vacuum gap. Hence the total mechanical force on the electrode may be expressed by :

$$F = \varepsilon_o V^2 A a^2/(2d_o^2) \qquad (2.3)$$

where F is the total force in Newtons and A the area of the electrode in m^2.

At low voltages, where the emission current is negligible, charging of the surface of the titania will not occur. Thus the voltage at the surface should be given by :

$$V_i = V/(1 + d_i/d_o k) \qquad (2.4)$$

where d_i is the thickness of the titania and 'k' is the relative dielectric constant of titania.

Hence $$a = 1/(1 + d_i/d_o k) \qquad (2.5)$$

It can be readily seen that since the relative dielectric constant for titania is about 95, 'a' will be approximately 1 until d_o becomes very small, say $d_o = d_i/10$. This theoretical value for 'a' will only be true for relatively low electric fields. Toso has shown that as the applied voltage is increased above a certain level the voltage across the vacuum gap tends to level off indicating a decrease in 'a'.

This change is clearly shown in figure 2.2 which has been adapted from Toso for the positive vacuum gap case. The fraction of the voltage dropped across the titania, (1 - a), is plotted against the voltage applied to the electrodes.

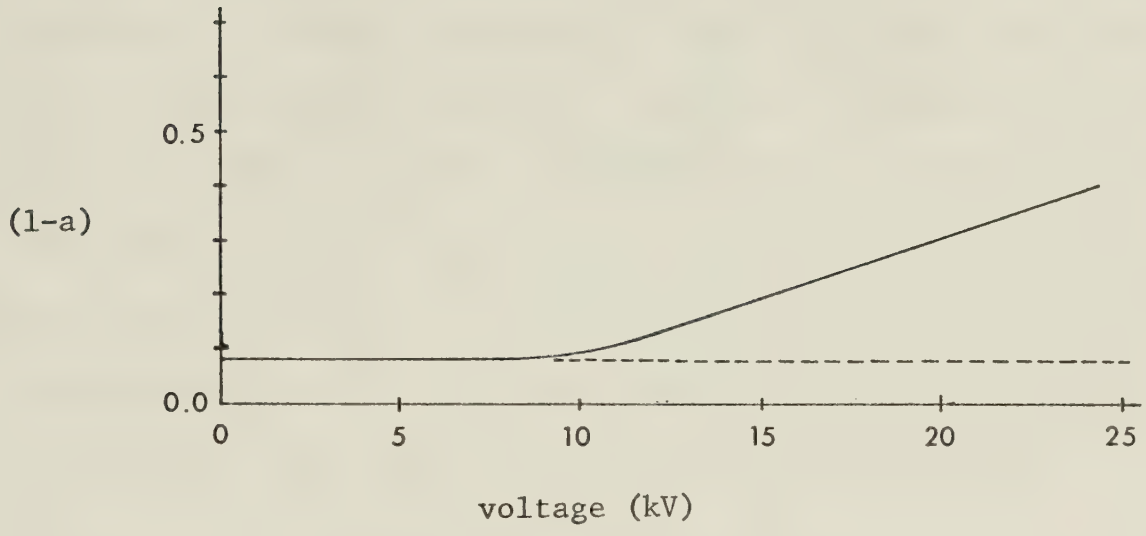

figure 2.2

This figure represents the case where d_o = 0.0015" (0.038cm) and d_i = 0.100" (0.254cm).

In order to measure 'a' it is necessary to express it in terms of experimentally measured parameters. By rearranging equation (2.3), one may obtain :

$$V^2/F = 2d_o^2/(\varepsilon_o A a^2) \qquad (2.6)$$

Thus the variation of V^2/F with voltage for a fixed electrode set-up is dependent on 'a'; hence any variation of 'a' from the theoretical value should be reflected in a variation of V^2/F.

3 EXPERIMENTAL APPARATUS

3.1 Measurement of force

It was decided to measure the force between the two electrodes or more correctly between the surface of the dielectric and one electrode by means of an electromechanical balance.

In principle, the balance (figures 3.1 and 3.2) consists of an arrangement of the two electrodes one above the other. The lower electrode is attached to the top of the vacuum manifold by an insulating tripod, the upper electrode is suspended from a solenoid. The titania sample is glued to the lower electrode with a conducting cement. Since the weight of the upper electrode is balanced by a spring holding it at an equilibrium position, the force applied by the solenoid is equal to the force due to the electric field across the vacuum gap.

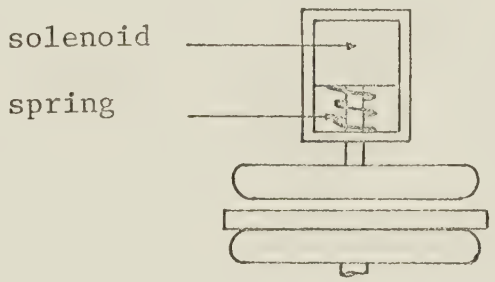

figure 3.1

The balance is set up by letting the upper electrode rest on the spring at its equilibrium position and then to bring down the solenoid until it is just touching the top of the thrust block.

The backing plate can then be loaded with weights and a relation obtained between the weight, i.e. the downward force and the current through the solenoid. This is done by holding the thrust block hard against the solenoid with a large current and slowly reducing the current until the upper electrode assembly dropped. This fall was stopped after

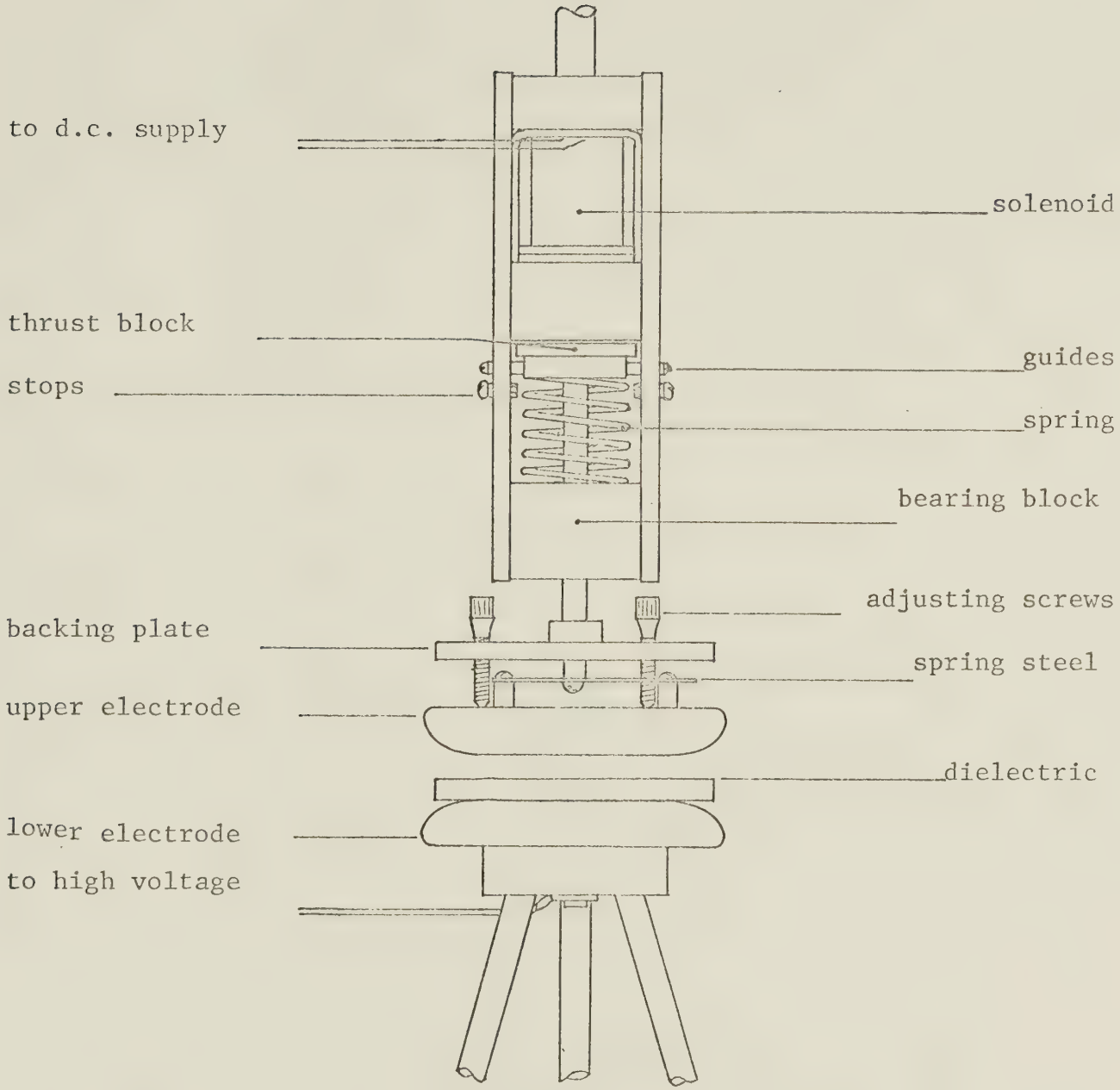
to d.c. supply
solenoid
thrust block
guides
stops
spring
bearing block
adjusting screws
backing plate
spring steel
upper electrode
dielectric
lower electrode
to high voltage

figure 3.2

a few thousandths of an inch by two stop - screws. The drop point was a definite point because as soon as the equilibrium was passed the electrode began to fall, pulling the plunger out of the solenoid and hence reducing the upward force. Due to this unstable equilibrium, it was easy, with a little practice, to obtain reproducible results consistent to about one percent over the period necessary for the calibration.

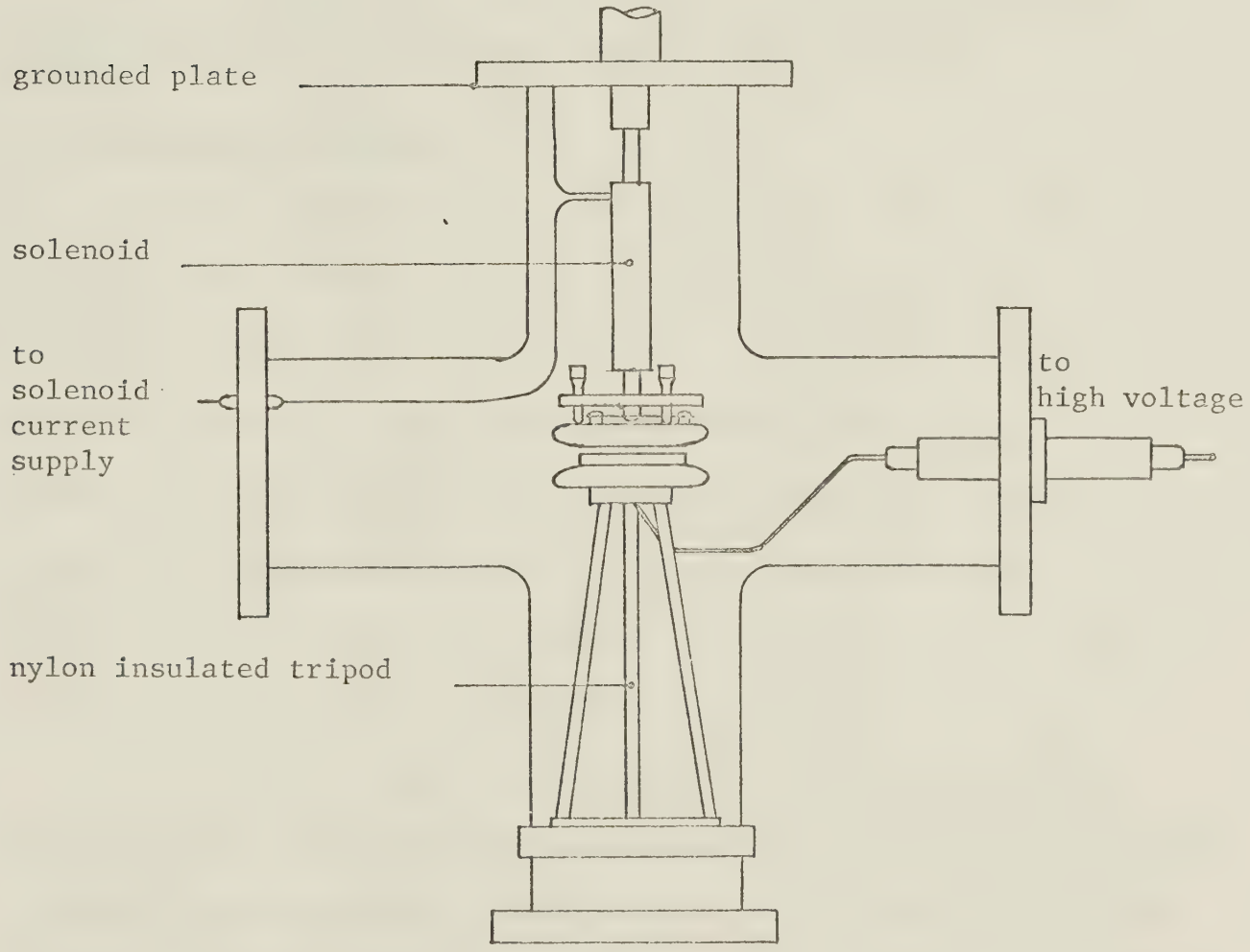

figure 3.3

3.2 Vacuum equipment

The entire solenoid balance was mounted in a glass cross as shown in figure 3.3. The pressure in the cross was kept at the order of 10^{-6} torr by the vacuum system shown in figure 3.4. The main pump was a two inch mercury diffusion pump. A water cooled baffle and a liquid nitrogen cold trap were used.

Pressure measurements were made using thermocouple gauges above 10^{-3} torr and a Bayard-Alpert gauge at lower pressures. The ultimate pressure of the system after it had been taken apart,cleaned and reassembled was slightly below 10^{-6} torr. All experiments were performed at pressures between 1 and 2 times 10^{-6} torr.

3.3. Electrical equipment

The high voltage was provided by a supply capable of giving voltages up to 50kV at currents up to 10mA with a voltage ripple of less than 0.2%. This supply was considerably modified by covering all possible breakdown points with corona shields, rebuilding resistor banks, increasing the spacing of components and finally building a new polarity reversing switch. The switch was made from perspex with sprung copper contacts as illustrated in figure 3.5. This switch allowed polarity changes to be made with the minimum delay.

The solenoid current was obtained from a Harrison 6204B d.c. power supply in the early experiments and a Power Designs 5015A supply in later experiments where greater current was required to raise the upper electrode. The current in both cases was measured on the same Weston ammeter.

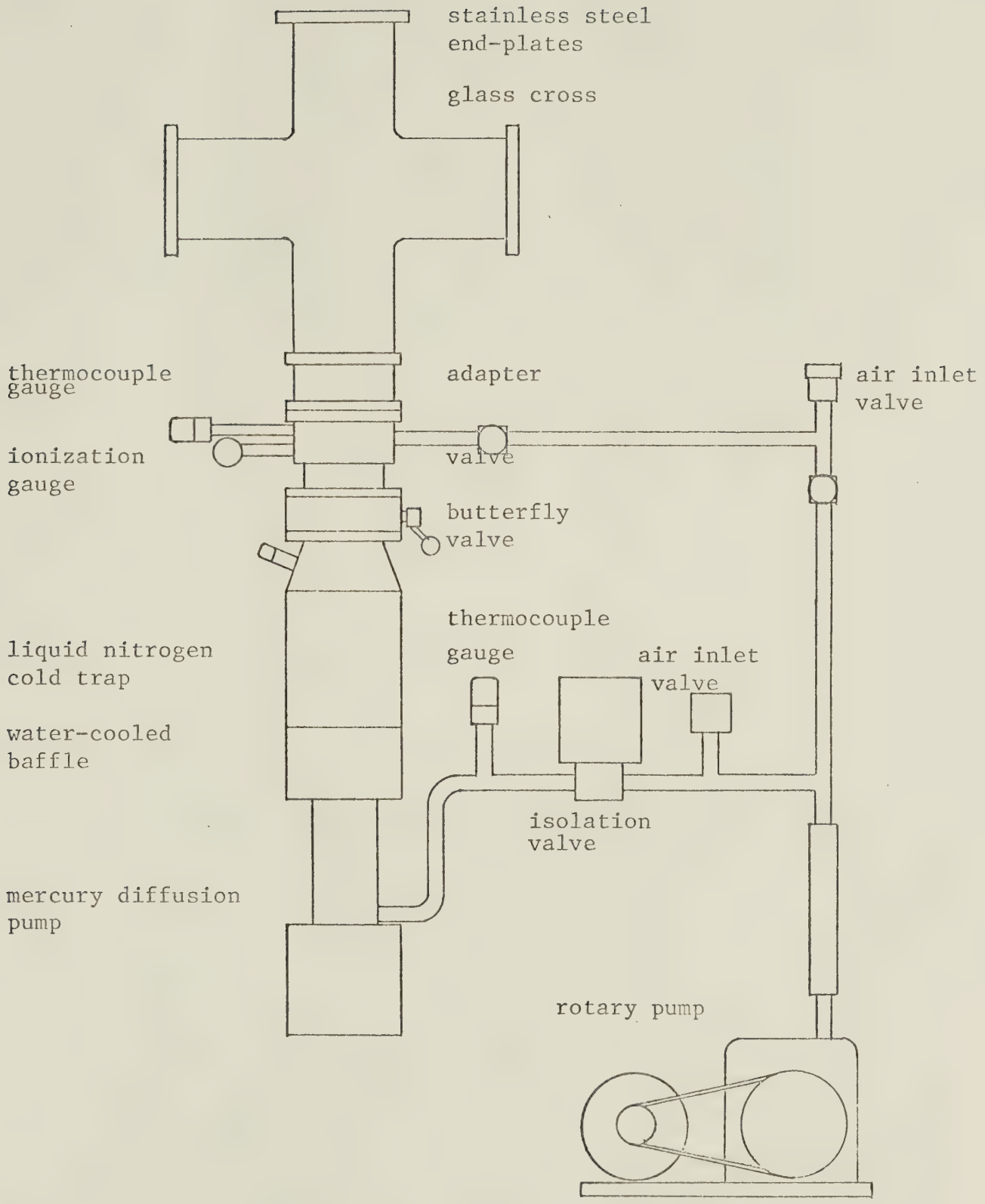

Vacuum system

figure 3.4

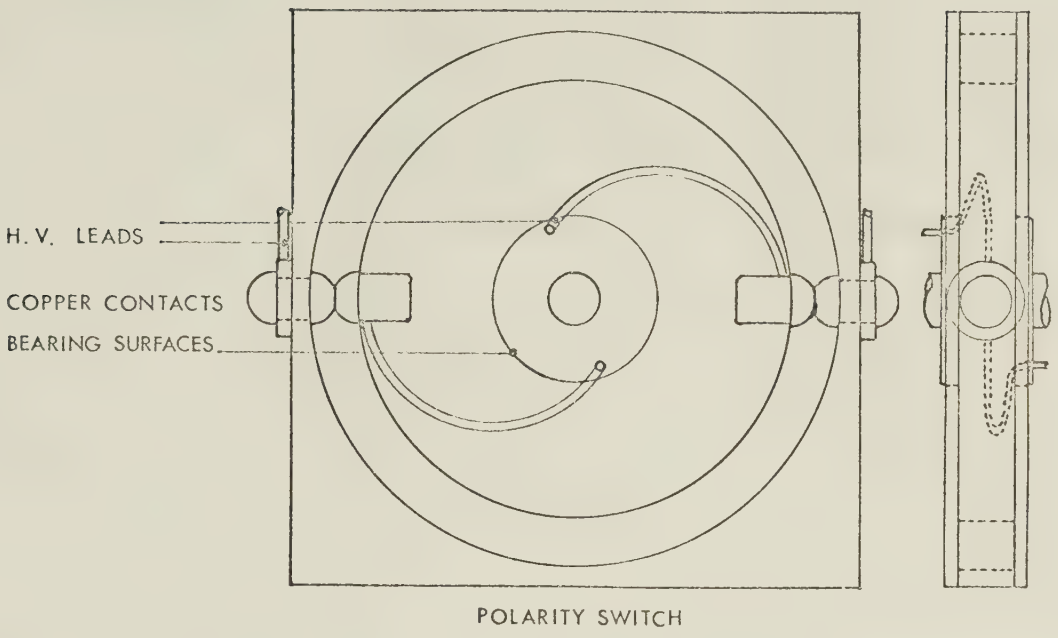

figure 3.5

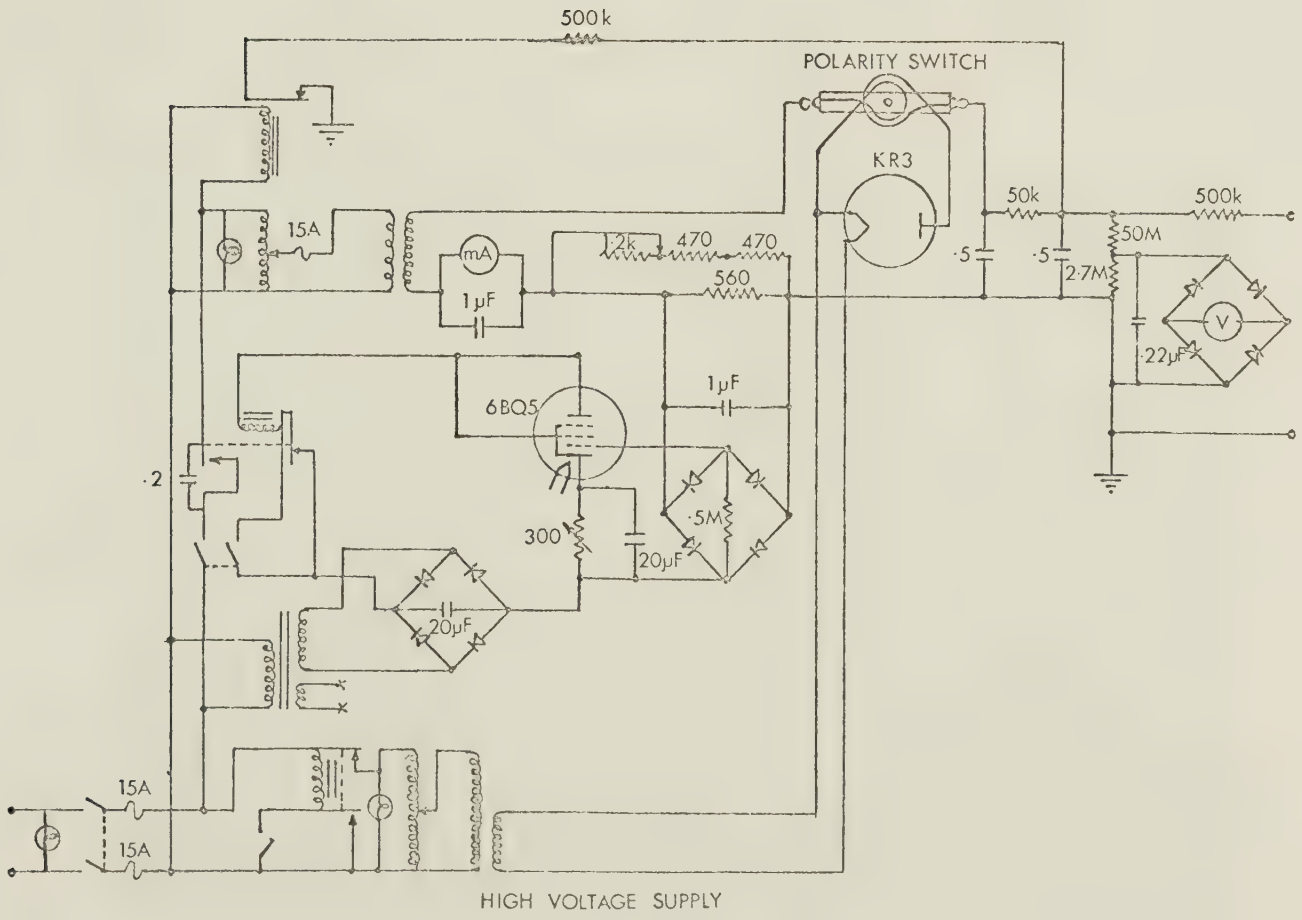

figure 3.6

4. EXPERIMENTAL PROCEDURE

4.1 Calibration

As a preliminary test of the solenoid-balance system in vacuo, it was decided to measure the force between two metal electrodes. It was thought that this would provide not only a useful calibration of the electrodes themselves, but also a check on the consistency of the apparatus over a wide range of field strengths and over a long time, since the results could be checked against theoretical predictions.

First the balance was calibrated against a set of balance weights as previously described. Then the force measurements were made and finally the balance was recalibrated.

Figure 4.1 shows a typical range of calibration curves. The force on the graph is given in grams since the solenoid was calibrated against a set of balance weights. For all calculations the force is converted into Newtons by means of the appropriate factors.

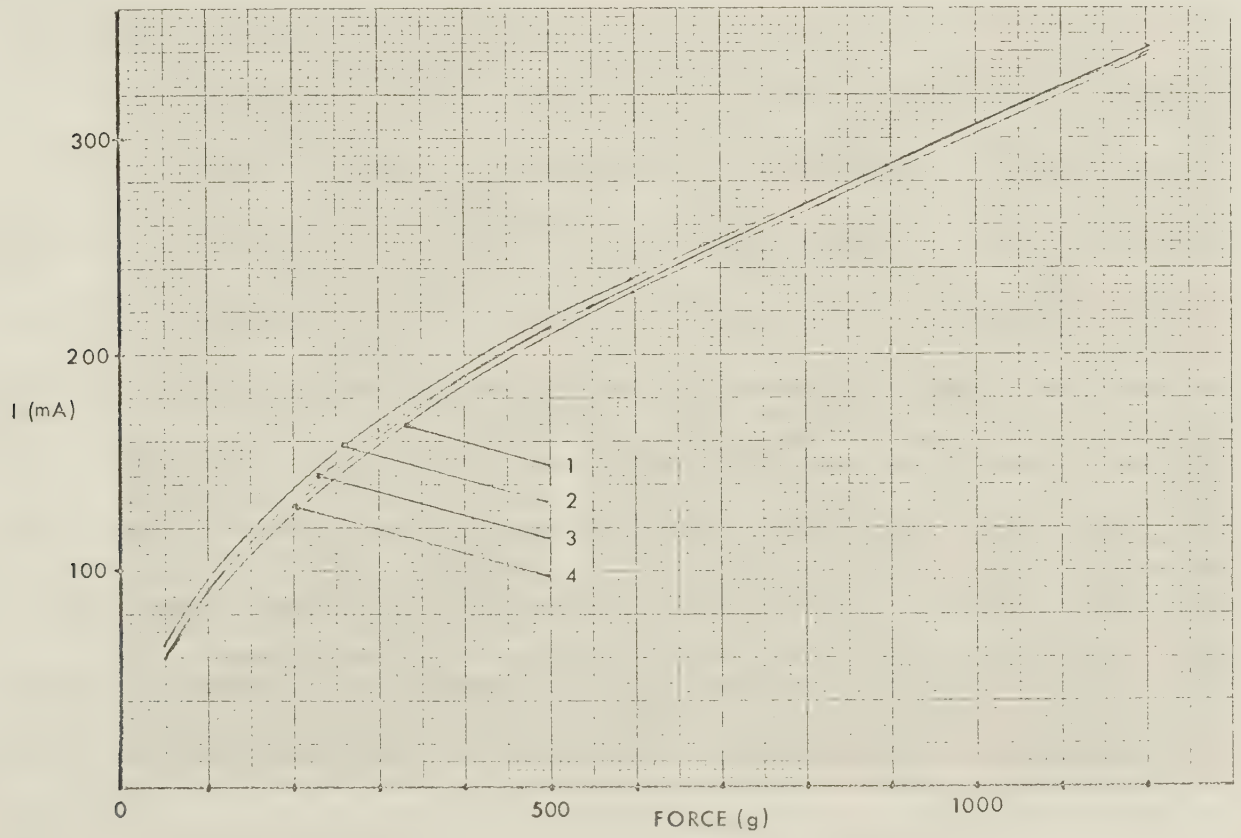

The four curves (1, 2, 3, 4,)represent calibrations taken over a period of some days with various measurements being done in between. The long term variations do not present too great a problem since one may interpolate the measurements between the appropriate calibrations. It is thought that the changes arise from a fatiguing of the spring which was only a coil of piano wire.

That the results obtained are essentially correct, is shown in figures 4.2 and 4.3. Figure 4.2 shows the relation between force and electrode spacing using curves of constant voltage. It may be seen from the graph that these curves have the expected property of being straight lines of slope -2. Similarly, figure 4.3, the plot of force against voltage for constant spacing has the expected slope of 2.

It may be concluded that the solenoid may be used to faithfully measure the characteristics of the force between two electrodes over a range between 10g and 1kg.

4.2 Electrode shape

Due to the need of mounting the entire dielectric within the flats of the electrodes in later experiments, it was decided to maintain this configuration throughout. Due to space limitations it was not possible to satisfy this condition using Bruce[5] electrodes. Electrodes of a somewhat similar shape but with a proportionately larger flat area were used. These electrodes were tested for breakdown in vacuo, as were a pair of Bruce electrodes of similar overall diameter. The breakdown voltages were essentially the same in both cases. Also, the breakdown voltages exceeded those expected from the data of Kilpatrick.[6](figure 4.4) Hence, it was concluded that the shape used gave rise to no field concentrations, otherwise a lower breakdown voltage would have been

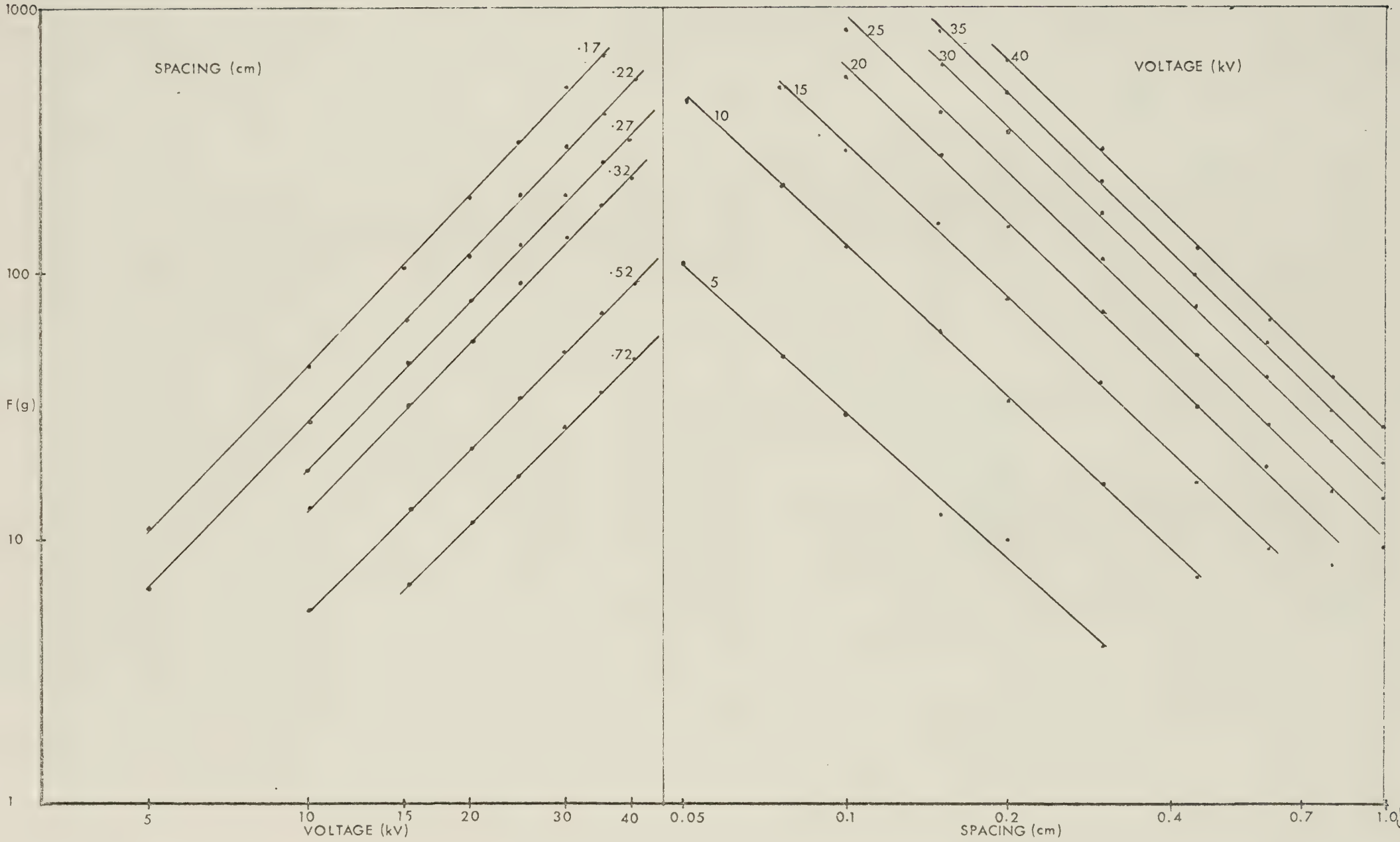
1000
100
10
1
F(g)
SPACING (cm)
·17
·22
·27
·32
·52
·72
5
10
15
20
30
40
VOLTAGE (kV)
VOLTAGE (kV)
25
35
30
40
20
15
10
5
0.05
0.1
0.2
0.4
0.7
1.0
SPACING (cm)

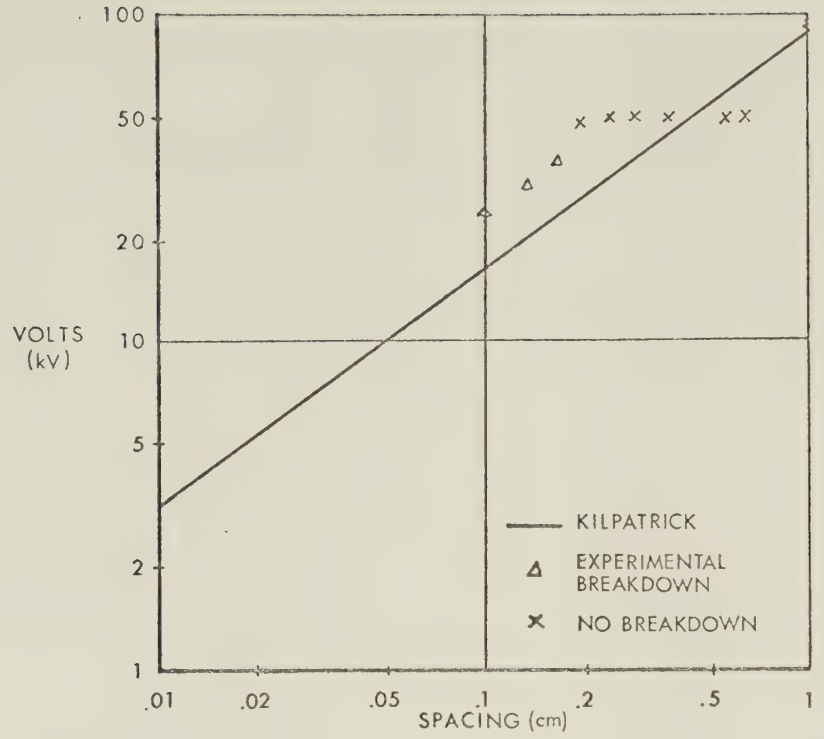

figure 4.4

observed.

4.3 Effective area

By using typical points from the curves one may obtain the effective area of the electrodes. Re-arranging equation (2.3), and setting $a^2 = 1$ (since there is no dielectric), one obtains :

$$A = 2Fd_o^2/\varepsilon_o V^2 \qquad (4.1)$$

Substituting all constants, and with F in grams and V in volts :

$$A = 22.15 \times 10^{-8} Fd_o^2/V^2 \qquad (4.2)$$

Taking values from figure 4.2, one obtains :

Volts (kV)	10	20	30	40
Area (cm^2)	32.1	33.8	35.4	34.6

yielding a mean value of $34cm^2$, which compares with $24cm^2$ for the flats of the electrodes and $54cm^2$ for the projected area of the electrodes.

Following these measurements, tests were done with the titania disc between the two electrodes. Using the procedures previously described, measurements were made over a range of vacuum gaps decreasing from 0.80cm. to a limit of 0.040cm. imposed by the operation

of the balance. Generally the voltage was increased in steps of 5kV except when near breakdown and for narrow gaps when 2kV increments were used. From these measurements and using equation (2.6), one may obtain plots of V^2/F for the various spacings. Any variation in 'a' will be reflected in V^2/F.

4.4 Effect of disc size

For practical reasons, it had been decided to use titania discs whose diameter was smaller than that of the electrodes. It was thought appropriate to check that the results from such an arrangement were compatible with those from the more usual case by taking measurements with both a 5cm. and an 8.2cm. diameter disc on 8.2cm. electrodes. From these tables and using a rearrangement of equation (2.6) one can calculate the effective areas of the two discs.

Vacuum gap (cm)	0.273	0.223	0.173	0.123
Large disc (cm^2)	42	40	40	37
Small disc (cm^2)	26	25	25	24
Small/Large	0.62	0.63	0.63	0.65

This ratio, approximately 0.63 between the effective areas of the two discs is in agreement with the measured areas of the two discs. The area of the small disc is $20cm^2$ and that of the large disc, taking the effective area measured previously is $34cm^2$ yielding a ratio of 0.59. Since the two cases are consistent in this respect and since a plot of V^2/F normalized to a common area coincides for the two discs, one may conclude that the two cases are equivalent and that one may treat the force from the small disc as being due entirely to the disc and ignore the peripheral area of the electrode. Hence the use of titania discs

smaller than the electrodes on which they are mounted is a valid procedure.

4.5 Surface finish

In order that the results of the force measurements could be carried over to the optical examination of the surface, all force measurements were carried out using dielectric samples which had been optically polished.

5. RESULTS

5.1 General procedure

Having established the validity of the technique, measurements were undertaken to establish the behaviour of V^2/F and hence 'a'. For the purpose of these calculations 'a' was assumed to have the theoretical value at low voltages allowing 'A' to be calculated which in turn provides a basis for calculating 'a' at higher voltages.

The general pattern of measurements was to start at a wide spacing and to continue with the same sample at decreasing spacings until breakdown occurred. After the electrodes had been repolished to remove the marks from their surfaces, a new piece of dielectric was inserted and measurements continued.

5.2 Large disc

After some initial runs to get the feel of the apparatus, tests were undertaken using the three inch diameter discs mentioned in section 4.2. These tests covered a vacuum gap ranging from 0.721 cm to 0.272 cm, in all cases going to 40 kV both positive and negative. No deviation from theoretical prediction was found, i.e. the plot of V^2/F was a straight horizontal line, nor were there any differences between positive and negative. This series of tests was continued to a spacing of 0.123 cm but with steadily decreasing maximum voltages until at this spacing breakdown occurred at 28 kV. The results of these tests are shown in figure 5.1. Since these results show no variation in V^2/F there can be no variation in 'a', so these results were used only to calculate the area 'A' in section 4.3. Tests were carried out at narrower spacings but these results cannot be considered since the lower electrode was pulled out of parallel due to the supporting tripod being inadequately secured.

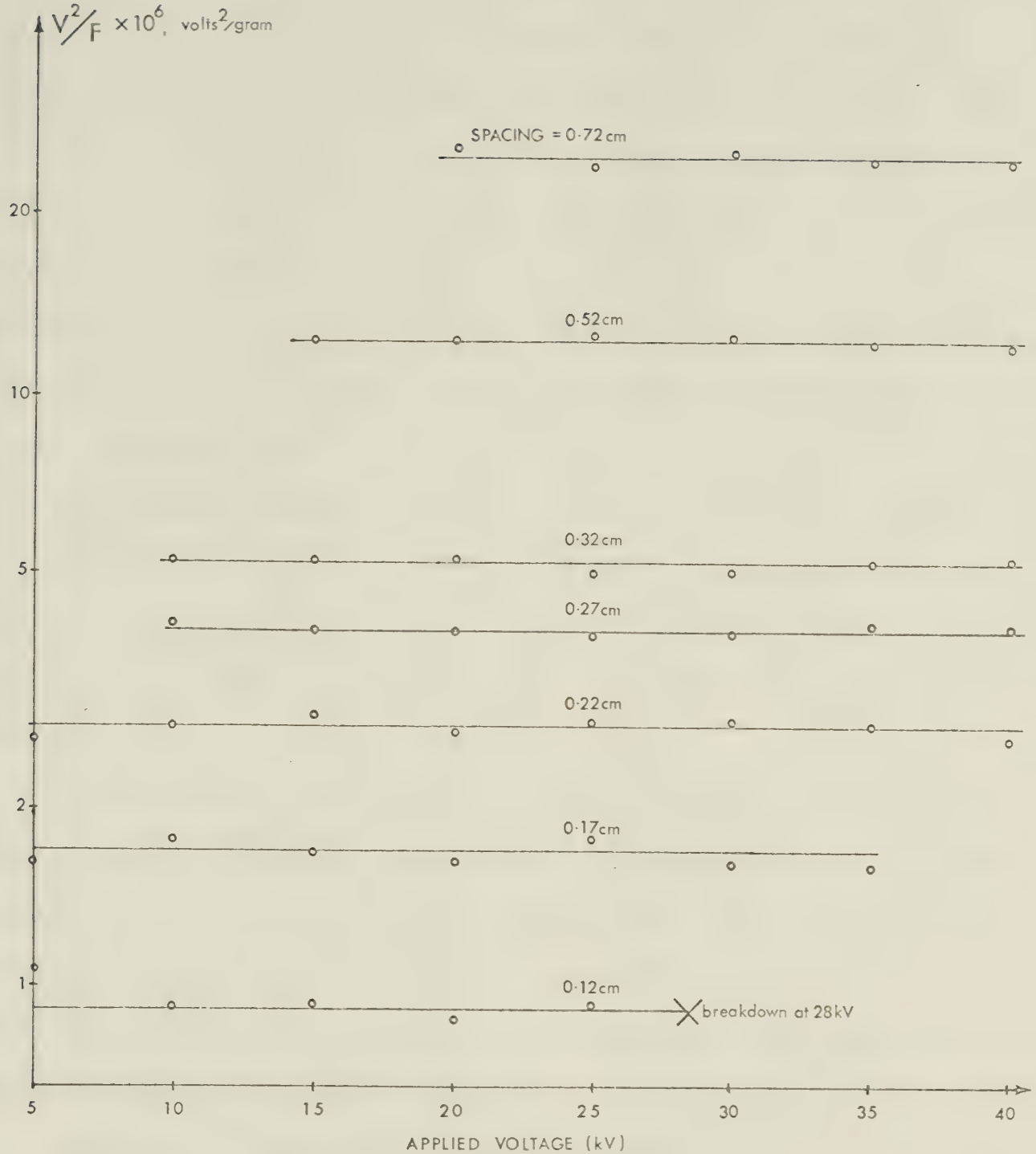
$V^2/F \times 10^6$, volts²/gram
SPACING = 0·72 cm
0·52 cm
0·32 cm
0·27 cm
0·22 cm
0·17 cm
0·12 cm
breakdown at 28kV
20
10
5
2
1
5
10
15
20
25
30
35
40
APPLIED VOLTAGE (kV)

figure 5.1

5.3 Small disc

The same pattern was followed in tests on the small discs with spacings ranging from 0.438 cm to 0.040 cm. Due to minor experimental problems breakdown occurred earlier than anticipated from previous work at the very small spacings. Once again measurements were repeated using both polarities at all spacings except the 0.040 cm where the last sample was destroyed on the positive vacuum gap case. Once again no difference between polarities was observed over the region covered. The tests from this group produced results that partly overlapped those obtained previously with the three inch discs. It was these results which were used to correlate the effect of the two disc sizes in section 4.4. The results of these tests are given in figure 5.2. In some cases, more than one test was done at virtually identical spacings. In plotting these results the data from the different tests are differentiated by different symbols.

It was thought that the cause of the breakdown at lower voltages than for Toso was caused by the sharp edges of the dielectric; so it was decided to round off the edge to a radius of about 1 mm. The first test with this edge was carried out at 0.053 cm with results as shown in figure 5.3. The radiused edge was successful in that 28 kV was reached before breakdown. All further tests were carried out using radiused discs.

This was the first test in which V^2/F and hence 'a' deviated from the horizontal. The results are slightly complicated by the need to stop the experiment on two occasions when the pressure due to the outgassing of the solenoid rose above acceptable levels. It will be seen from figure 5.3 that once a certain value of V^2/F had been reached it did not

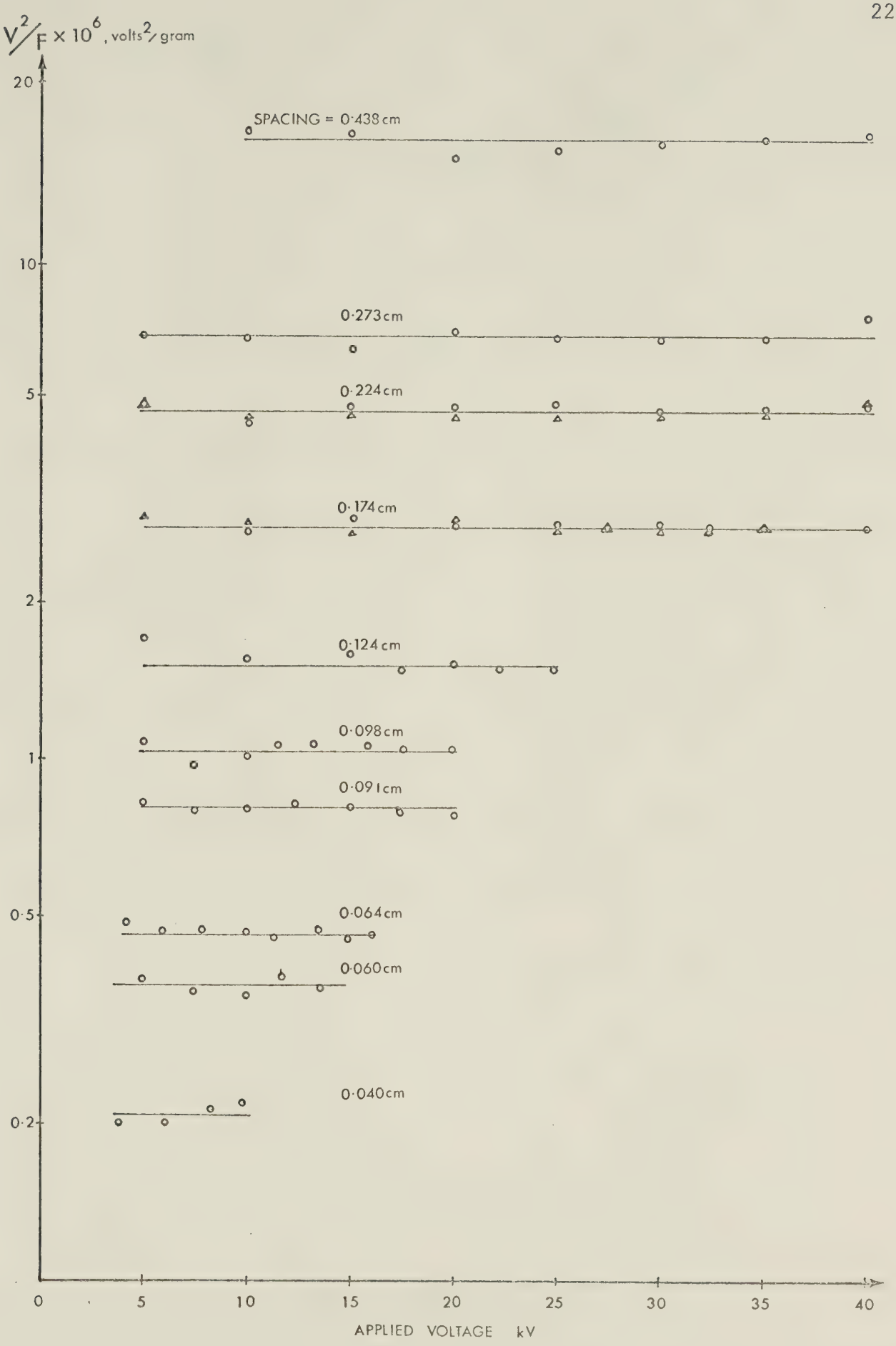
$V^2/F \times 10^6$, volts^2/gram
20
10
5
2
1
0·5
0·2
SPACING = 0·438 cm
0·273 cm
0·224 cm
0·174 cm
0·124 cm
0·098 cm
0·091 cm
0·064 cm
0·060 cm
0·040 cm
0
5
10
15
20
25
30
35
40
APPLIED VOLTAGE kV

figure 5.2

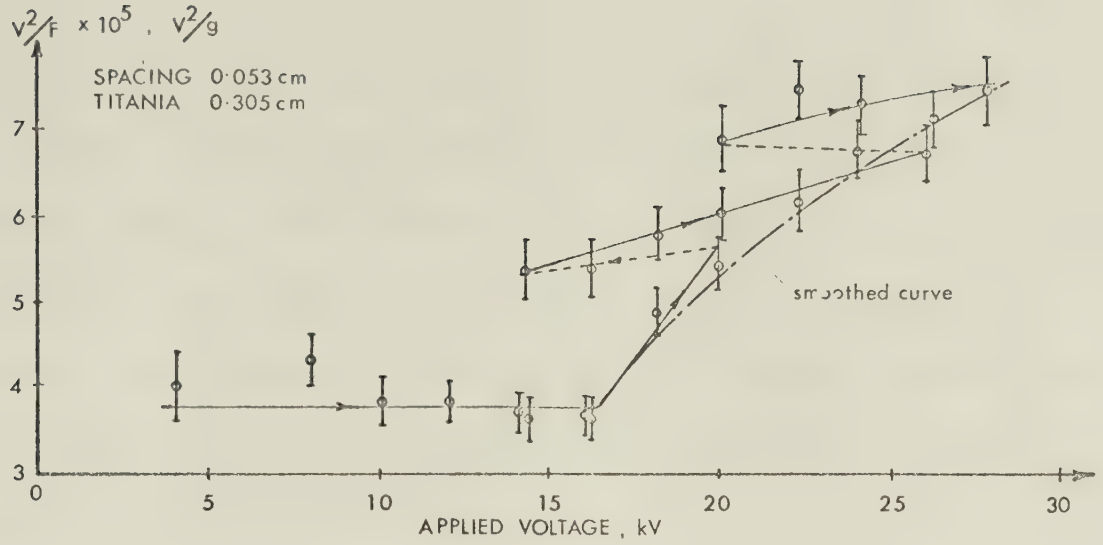

figure 5.3

go down when the voltage was reduced. This effect poses two possibilities: either there has been some permanent change in the properties of the titania or there is some residual surface charge on the dielectric. In order to distinguish between the two possibilities, an experiment was performed in which the voltage was increased to a fairly high voltage (20kV) then decreased back to zero. Following that, every effort was made to discharge the surface by letting the vacuum chamber up to atmosphere and temporarily reversing the polarity. Finally, the experiment was repeated. The results are seen in figure 5.4

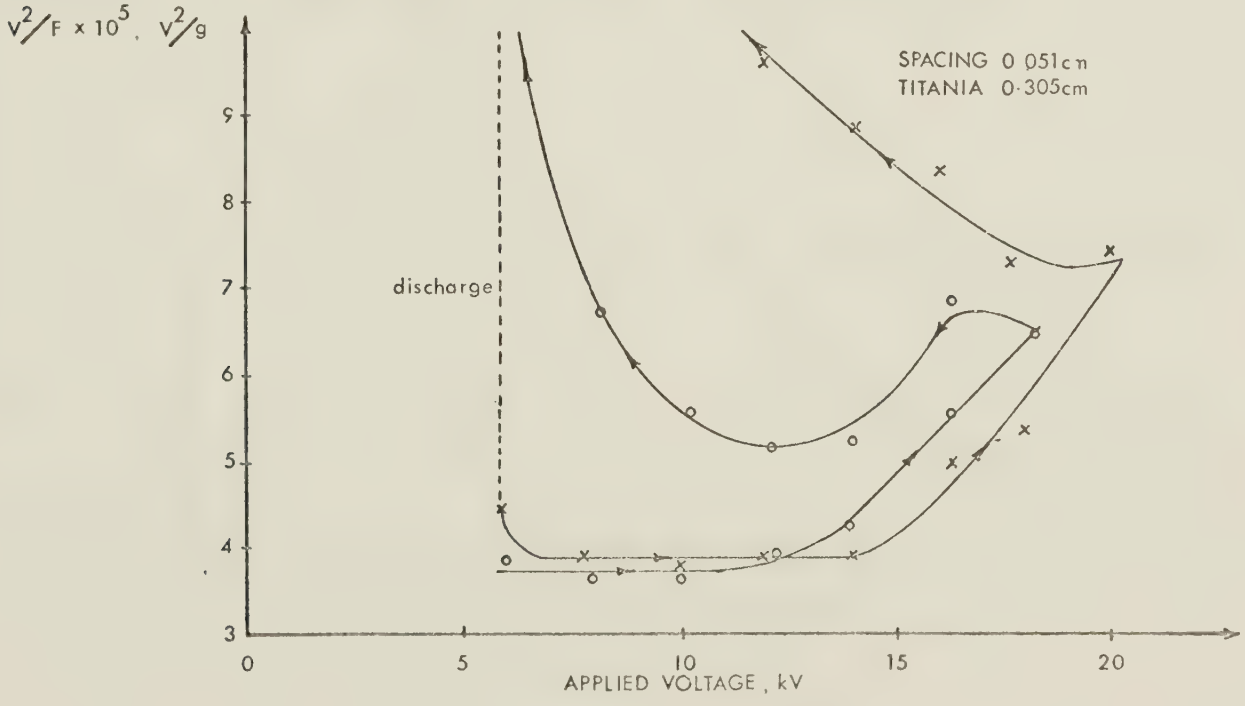

figure 5.4

It can be seen from this figure that on the run-down the value of V^2/F varied somewhat but generally increased as would be expected if some of the charge remained on the surface. If all the charge generated at the highest voltage remained on the surface then the curve would rise continuously with decreasing voltage to values somewhat higher than those realized. Since it proved possible to repeat the experiment with reasonable accuracy after discharging the surface, it may be concluded that the titania stores surface charge for a considerable time but that there is no permanent change in the properties of the titania.

A curve is drawn on figure 5.3 through the values of V^2/F obtained when it was measured for the first time at each voltage. From this smooth curve points are taken for the calculation of 'a'. A value of 0.37×10^6 volts^2/g was used to arrive at a value of 19 cm^2 for the area. As expected this is slightly smaller than previous values of 'A' due to the rounding of the edges. One may then determine 'a' from :

$$a^2 = 3.25 \times 10^5 \frac{F}{V^2} \qquad (5.1)$$

The results of these calculations are shown in figure 5.5.

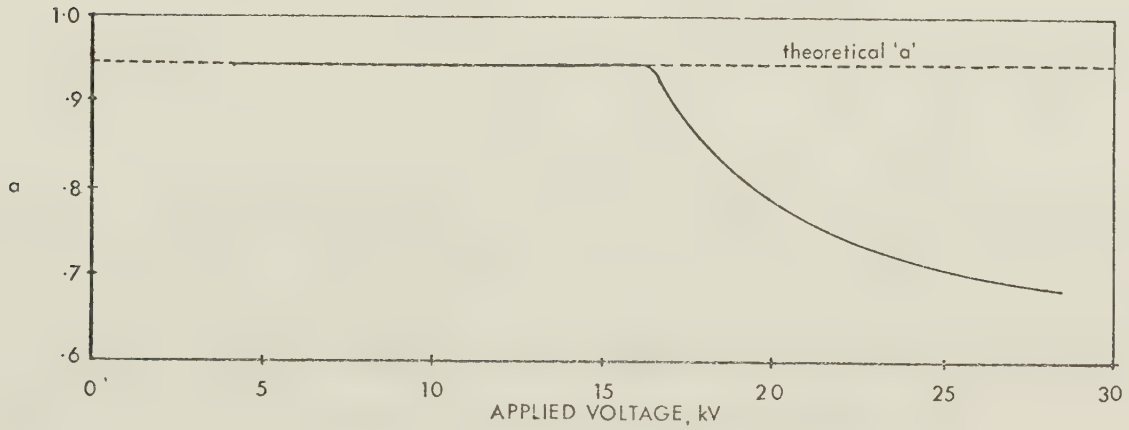

figure 5.5

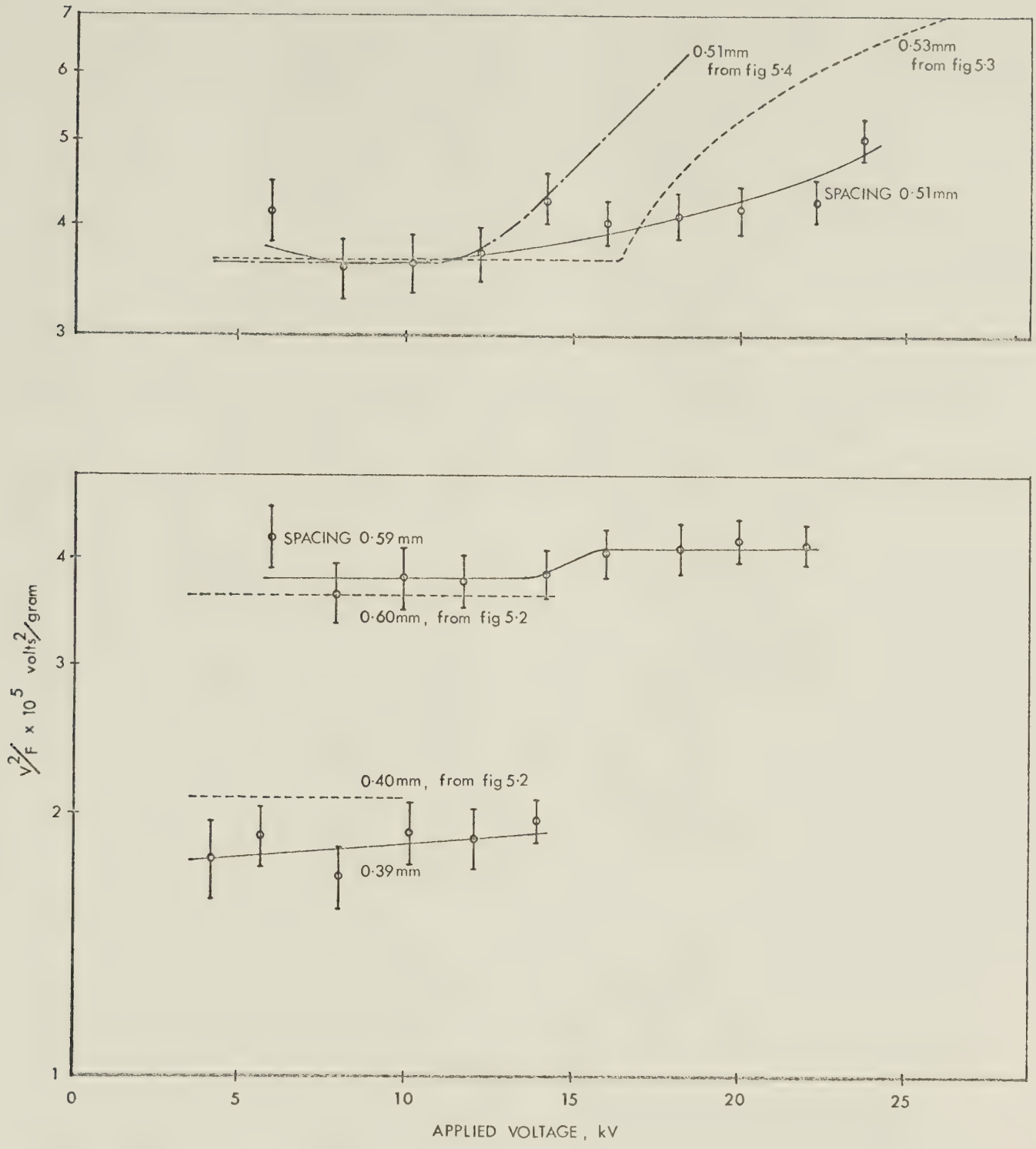

Figure 5.6. Results of measurements across small vacuum gaps for positive vacuum gap. Dotted curves represent results from earlier experiments. Results for the 0.051 cm gap overlap those of the 0.059 cm gap; so, for the sake of clarity, the 0.051 cm case is shown separately.

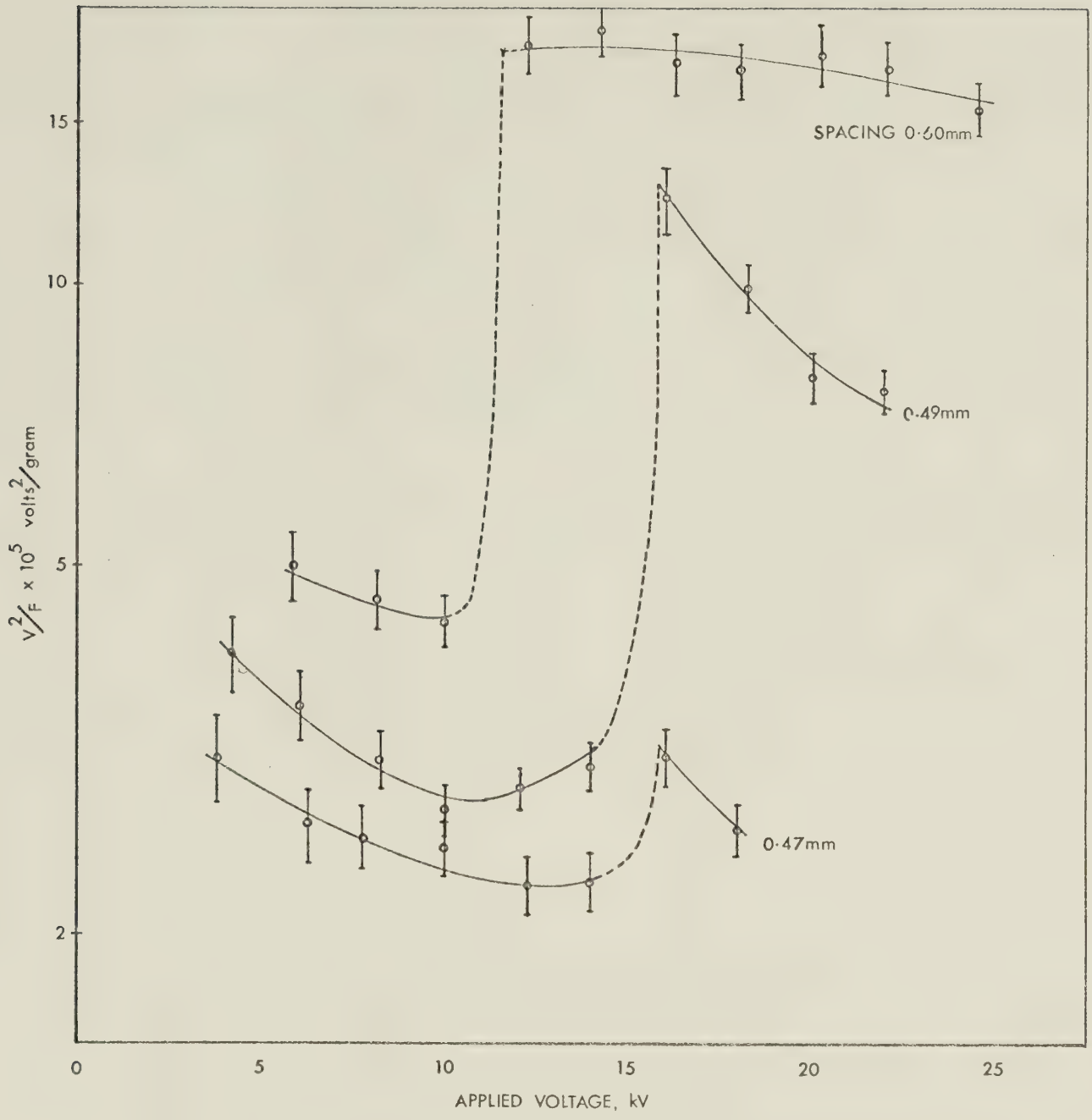

Figure 5.7. Results of measurements across small vacuum gaps for negative vacuum gap (ceramic anode). That part of the curve between the two levels is shown dotted since behaviour in this region can only be speculative. The sample at 0.049 cm is one of the speckled discs; the other two, regular surfaces.

Further tests were done at close spacings using dielectric with radiused edges. Unfortunately the first batch used was covered with black speckles. It was thought that these speckles may have been iron particles imbedded in the titania when it was being lapped on an iron plate. However the speckles did not disappear when the titania was soaked in heated acid. This was the only time titania was polished in this fashion. Of the four pieces used three were used as cathodes (see figure 5.6) and one as an anode (figure 5.7). The cathode case was much as expected but the anode showed a surprising jump in V^2/F rather than the gradual rise previously encountered. In case this should be due to the possible iron in the surface, the experiment was repeated twice with samples polished as usual on glass. As can be seen from figure 5.7 similar behaviour resulted. In exactly the same manner as before 'a' was calculated and is shown in figure 5.9.

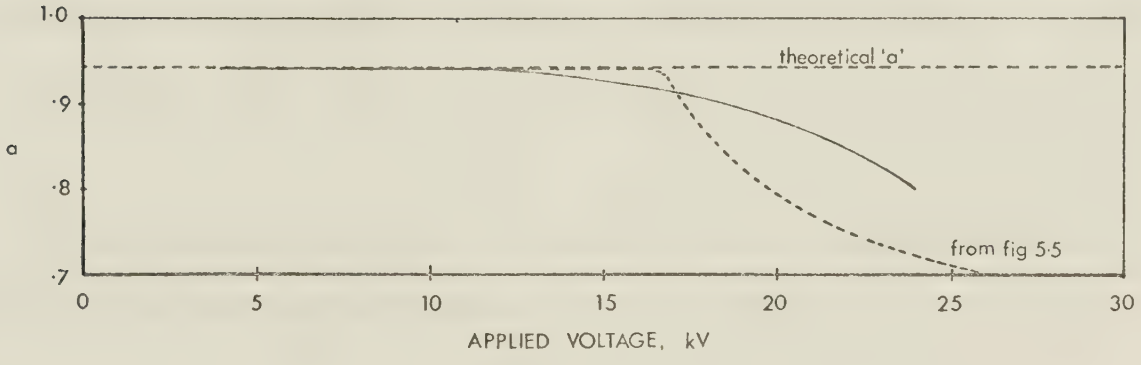

figure 5.8. 'a' for the positive vacuum gap (ceramic cathode)

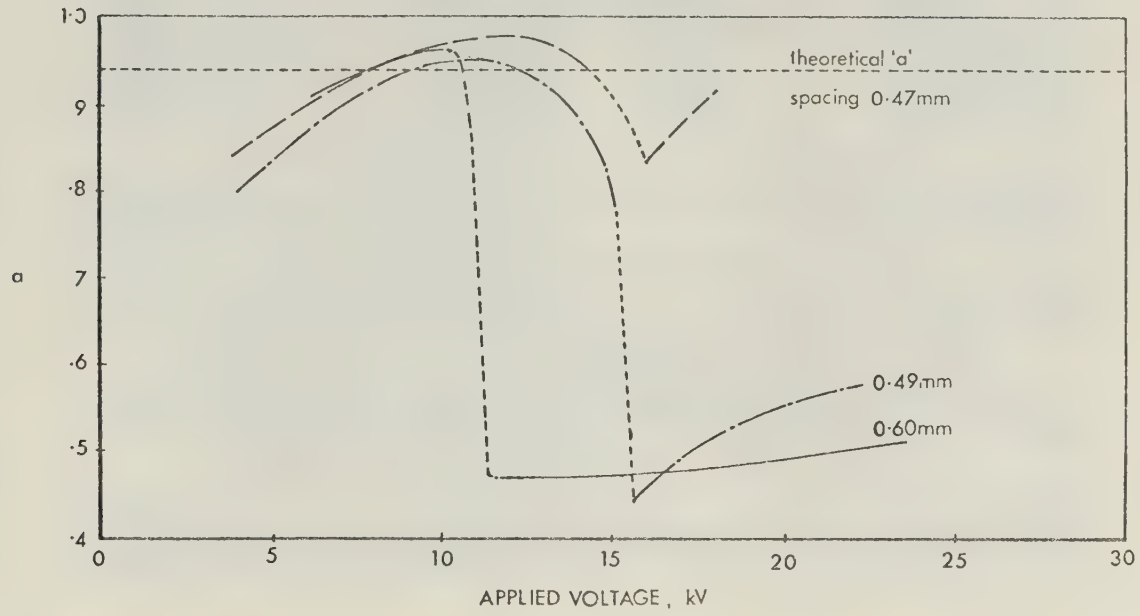

figure 5.9, 'a' for the negative vacuum gap (ceramic anode)

5.4 Visible effects

An interesting phenomenon was observed in the breakdown at close spacings. It was noted that after breakdown there was a column of material joining the dielectric to the upper electrode. This was photographed and is shown in figure 5.10. This photograph has been taken through the walls of the cross which cause the distortions, unfortunately this procedure was necessary because the column was so fragile that it usually collapsed while the endplate was being removed from the cross to take a picture looking through the end. On examination the material of the column appeared to be small pieces of titania which had been chipped from the surface and reduced.

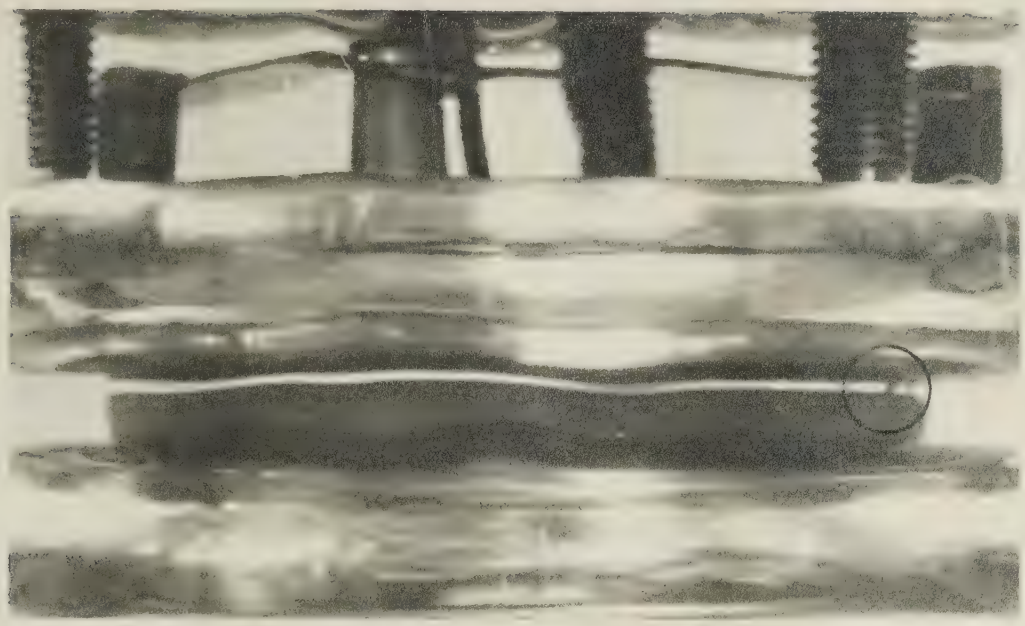

figure 5.10

5.5 Estimate of errors

In order to estimate the size of the errors it is necessary to carefully consider the methods by which the results were obtained. Consider the force measurement; if a typical calibration curve is examined it will be seen that the RMS deviation of the experimental points from the curve is approximately 2%. In the measurement of the force itself it is reasonable to expect an accuracy of ± 2mA, a fifth of the smallest division. This would give a reading error of hyperbolic form. The total error in the force measurement may be considered to be the sum of these two errors. In the case of the voltage, the voltmeter may be read to an accuracy of ±2% in the voltage calibrator against which the meter is ultimately compared.

Hence the maximum error in V^2/F is given by:

$$E_{V^2/F} = \sqrt{(2E_V)^2 + E_F^2} \qquad (5.2)$$

As can be seen from the error bars on the graphs this can range from 13% at low voltages and forces to 5% under favourable conditions.

From an examination of figure 5.2, it will be noted that for the spacings 0.223 cm and 0.175 cm where the tests were repeated, the experimental points fall within each other's error limits. Hence one may conclude that the error limits thus obtained are reasonable. Agreement is not quite as good at the very close spacings, but this is because of the increasing importance of uncertainties in d_o which may be of the order ±3%. Also the fact that surface phenomena due to local irregularities are being investigated means that variations between samples are not unexpected.

6. SUMMARY OF FORCE MEASUREMENTS

The results outlined in section 5 do not agree very closely with the work of Toso. Figure 6.1 compares the result given by Toso for a positive vacuum gap of 0.015 inches (0.04 cm) with the results in figures 5.5 and 5.8 for a vacuum gap of 0.05 cm.

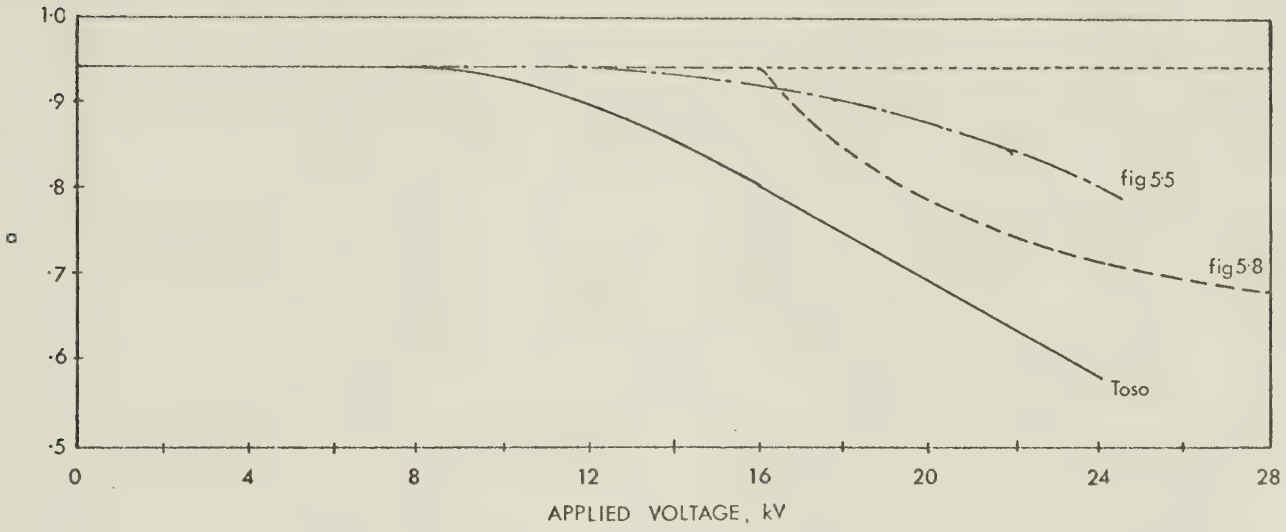

figure 6.1

These results are not directly comparable since they are for different spacings, however, the figure will serve to illustrate the general trends. It is not surprising that Toso's curve should give lower values after the knee because of the narrower spacing. The most noticeable factor is the difference of the two curves in the present experiment. Since these two tests were on different specimens this difference is not surprising; what is reassuring is that generally the same type of behaviour is encountered. It is unfortunate that tests at the narrower spacing of 0.04 cm resulted in breakdown before any anomalous behaviour was observed.

Figure 6.2 is a similar comparison for the negative vacuum gap (ceramic anode) case. It may be seen in this drawing that there is very

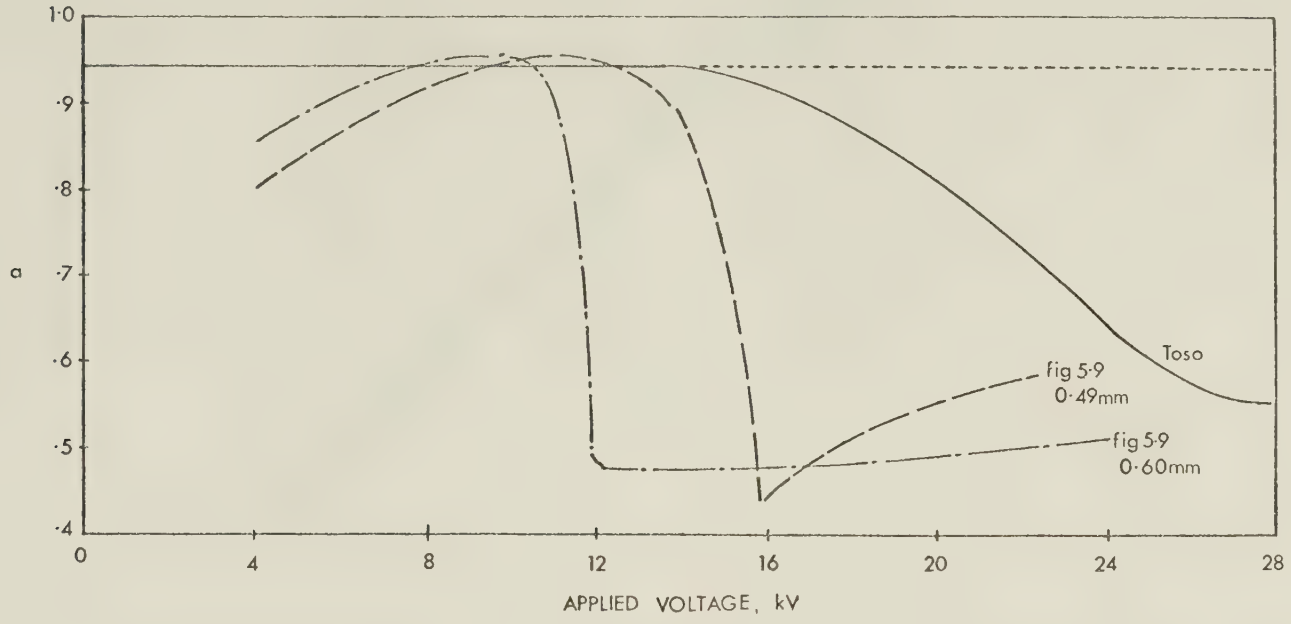

figure 6.2

little similarity between the results of Toso and those of the present experiment. Surprisingly, the break point of the curve i.e. that point where the curve deviates from the horizontal, has moved lower with increased spacing, exactly the opposite from what would be expected.

Although the differences in figure 6.1 may be reconciled due to the different samples used, the differences in figure 6.2 are of such a nature that some fundamentally different mechanism must be at work. It is interesting to note that in Toso's experiment the break point occurred at a lower voltage in the positive vacuum gap case whereas in the present experiment, the reverse was true.

It can only be concluded from these results, that a great variation in behaviour is possible between different samples. The results of the present work would suggest a different cause of these deviations from theoretical behaviour depending on the polarity used.

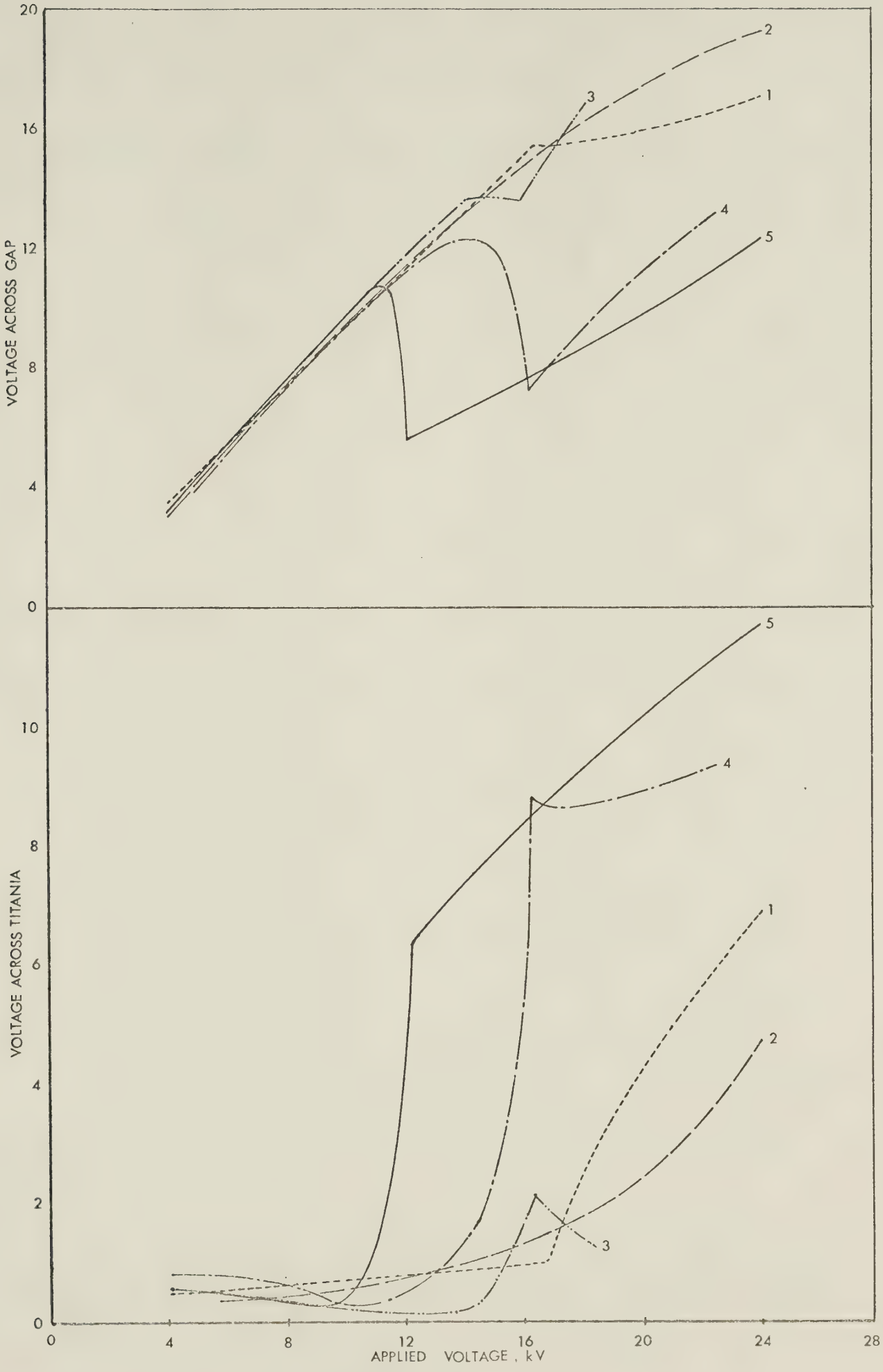
VOLTAGE ACROSS GAP
VOLTAGE ACROSS TITANIA
APPLIED VOLTAGE , kV
0
4
8
12
16
20
24
28
1
2
3
4
5

figure 6.3.

Figure 6.3 shows the dependence of the voltages across the vacuum gap and the ceramic on the voltage applied.

Experiment Number	1	2	3	4	5
Breakdown (kV/cm) Ceramic	23	16	4	30	39
Vacuum	320	370	350	260	200

Experiment Number; 1 positive gap, 0.053 cm

2 0.051 cm

3 0.047 cm

4 negative gap, 0.049 cm

5 0.060 cm

It will be noted that for the three ceramic cathode runs breakdown occurs at about the same level of electric field intensity in the vacuum gap, but that there is a wide variation in the intensity across the titania. In fact the total voltage at breakdown across the vacuum gap is very similar in all three cases, ranging from 16.7 to 19.1 kV. A similar state of affairs exists for the ceramic anode case where the voltages across the gap are almost identical being 12.8 and 12.2 kV. In this case however, the field intensities across the ceramic and vacuum gap show equal but opposite variation. The behaviour of $V_{ceramic}$ is in general agreement with the results of Englefield et al. which showed breakdown at 30 kV/cm for the ceramic cathode and 43 kV/cm for the ceramic anode.

The voltage across the vacuum gap and the electric field intensity are considerably greater for the positive vacuum gap (ceramic cathode) than for the ceramic anode case. Since many workers consider that the

breakdown is dependent on the anode material, this is not surprising, although it is not in agreement with Toso's work.

It should be noted that in all cases the breakdown voltage exceeds that predicted by Kilpatrick for the spacings used if metal electrodes had been employed.

PART II

INTERFEROMETRIC OBSERVATION OF BREAKDOWN ON DIELECTRIC SURFACES

7. MULTIPLE-BEAM INTERFERENCE

7.1 Introduction

The intention of this project was to investigate local variations in field strength and their effects on a dielectric surface which might arise prior to breakdown. The purpose of the preliminary experiments described thus far was merely to better establish one of the parameters, namely the average field across the dielectric as distinct from that given by theory.

Due to the high field strengths involved and the small dimensions of the vacuum gap, the use of any material type of probe is precluded. One mechanism which immediately suggests itself is the use of interferometry which has long been used as a technique for ascertaining the flatness of surfaces. The advent of the laser removes one of the worst restrictions of the technique which previously limited work to gaps of a maximum of about 0.5mm. With the laser one can easily get fringes between plates with centimeter spacings.

Simple interferometers using air-glass interfaces are limited in resolution in that only the first reflected beam is strong enough to contribute to the image. In a multiple beam interferometer, metal coatings having a high reflectivity are used to enhance the subsequent reflected beams which greatly increase the sensitivity of the apparatus.

7.2 Airy's formula

The theory of multiple-beam interference taking place between two plane parallel surfaces was first derived by Airy but did not find application for many years. By multiple beams is meant the use of a series of coherent beams all specifically related in phase and intensity. Airy had calculated the result of considering the successive multiple

beams as shown in figure 7.1.

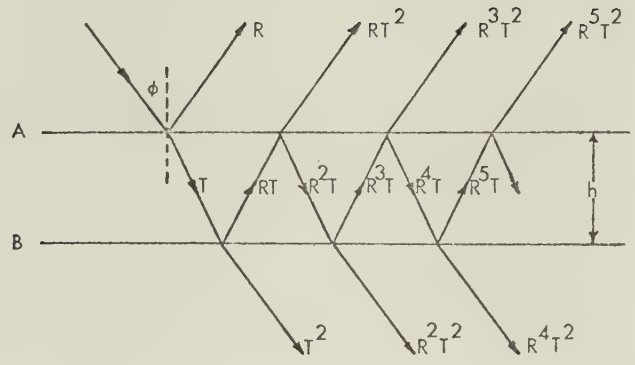

figure 7.1

From figure 7.1, it is clear that the reflected beams will have intensities R, RT^2, R^3T^2, R^5T^2, ... etc. If these are collected by a lens, all the beams will combine at the focus of this lens. Now each successive beam lags behind the previous beam a distance $2\mu h\cos\phi$, in which 'ϕ' is the angle of incidence and 'h' the distance between the parallel surfaces. The phase lag 'δ' between successive beams is constant being

$$\delta = \frac{2\pi}{\lambda} 2\mu h \cos\phi \qquad (7.1)$$

If the reflected series of beams of geometrically decreasing intensity (decreasing by a factor R^2) and phase increasing arithmetically by δ is summed to infinity, the resulting intensity at any point in the field corresponding to δ can be shown to be [7,8]:

$$I = \frac{4R\sin^2\delta/2}{(1-R)^2+4R\sin^2\delta/2} \qquad (7.2)$$

This represents Airy's formula for reflected intensity. The quantity $\sin^2\delta/2$ can only vary from 0 to 1, at which I has minimum and maximum values respectively. When $\sin^2\delta/2=1$

$$I_{max} = \frac{4R}{(1-R)^2+4R} \qquad (7.3)$$

which simplifies to $4R/(1+R)^2$. For fairly large values this is always nearly unity. For example:for R=0.9 it equals 0.997, even for R=0.6 it still equals 0.94. Also it should be noted that the minima do not really go down to zero (true only when there is no absorption). Effectively the maxima can be treated as unity, irrespective of the reflection coefficient, and the minima as zero. In practice this condition breaks down because of the absorption of the reflecting film.

7.3 Fringe width

The intensity distribution of the reflected light pattern given by (7.2) may be written as

$$I = \frac{F\sin^2\delta/2}{1+F\sin^2\delta/2} \qquad (7.4)$$

where the parameter F is defined by the formula

$$F = \frac{4R}{(1-R)^2} \qquad (7.5)$$

When R is small compared with unity, F is also small compared with unity, so one may expand $1/(1+F\sin^2\delta/2)$ in (7.4) and retain terms up to only the first power in F. This gives

$$I \simeq \frac{F}{2}(1-\cos\delta) \qquad (7.6)$$

i.e. the intensity variations are characteristic of two interfering beams. If R is increased, the intensity of the maxima approaches unity and the minima become sharper until, when R approaches unity so that F is large, the intensity of the reflected light is very bright except in the vicinity of these minima. The pattern in reflected light becomes one of narrow dark fringes on an otherwise nearly uniform bright background. The behaviour of I as a function of the phase difference δ is shown for various values of F in figure 7.2

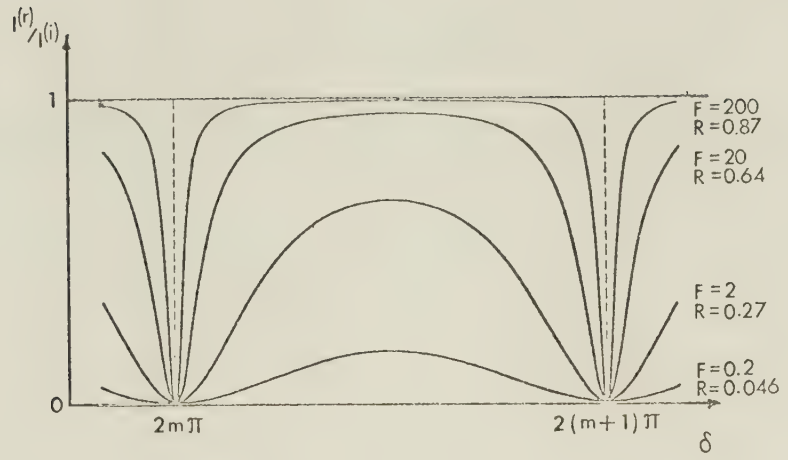

figure 7.2

The sharpness of the fringes is conveniently measured by their half intensity width, or 'half width', which, in the case of the pattern in reflected light, is the width between the points on either side of a minimum where the intensity has risen to half its maximum value. The ratio of the separation of adjacent fringes and the half width is known as the 'finesse' $\mathcal{F}$ of the fringes. For a fringe of integral order 'm', the points where the intensity is half its maximum value are at

$$\delta = 2m\pi \pm \frac{\varepsilon}{2} \tag{7.7}$$

where by (7.3) and (7.4)

$$\frac{2R}{(1+R)^2} = \frac{F \sin^2 \varepsilon/4}{1+F \sin^2 \varepsilon/4} \tag{7.8}$$

and when F is sufficiently large, δ is so small that one may put $\sin(\varepsilon/4) = \varepsilon/4$ in (7.8) and obtain the half width as

$$\varepsilon = \frac{4\sqrt{2}}{\sqrt{F}} \sqrt{\frac{R}{1+R^2}} \tag{7.9}$$

Since the separation of adjacent fringes corresponds to a change 2π of δ,

the finesse is then

$$\mathfrak{F} = \frac{2\pi}{\varepsilon} = \frac{\pi\sqrt{F}}{2\sqrt{2}}\sqrt{\frac{1+R^2}{R}} \qquad (7.10)$$

As R approaches closer to unity (7.10) may be simplified to the more usual expression

$$\mathfrak{F} = \frac{\pi\sqrt{F}}{2} \qquad (7.11)$$

All these formulae have been derived for the case where the two reflecting coefficients are equal. If the reflecting coefficients of the two surfaces differ and are R_1, R_2, the formulae given above hold if R is replaced everywhere by $\sqrt{(R_1R_2)}$ [9].

7.4 The effect of absorption in the metal film

In the reflected system the calculation of the effect of absorption is quite complex, yet one can see in a general manner what happens by an argument due to Tolansky.[8] In figure 7.1 one sees that the absorption in the metal film does not affect the first beam of intensity R. It does affect every succeeding beam. The intensity of the second reflected beam is RT^2, but the transmission is no longer (1-R) but is reduced to (1-R-A) where A is the absorption. The result of this is that the sequence of reflected beams, which produce the dark interference fringe, is weakened, and as a consequence the fringe minimum does not go down to zero. The greater the absorption the more the fringe is affected. The effect is shown schematically in figure 7.3. In figure 7.3a, with moderately low reflectivity and low absorption the fringes are broad but visibility is fairly good, i.e. the fringes dip down low. In figure 7.3b the reflectivity is high, with sharp fringes, but absorption increases

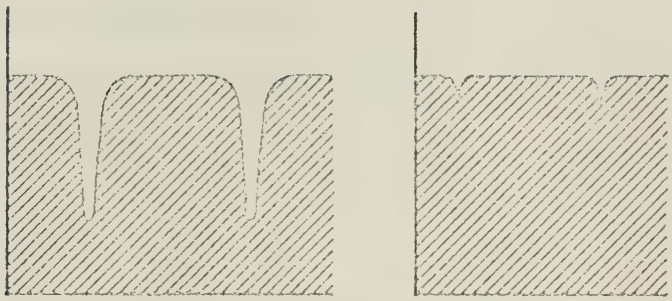

(a) (b)

figure 7.3

with higher reflectivities, consequently the fringe dip is only slight and visibility is poor. The fringes are narrow but hard to see.

8. EXPERIMENTAL APPARATUS

8.1 Fabry-Perot Interferometer

A typical Fabry-Perot interferometer is used as shown in figure 8.1. Since the laser provides a light beam approximately 1mm diameter, it is necessary to use a short focal length lens to diverge the beam in order that it may cover the region of interest. The diverging lens and a pinhole are mounted together as one unit which is movable with respect to the collimating lens. This allows fine adjustments to be made for focus. The lens must be kept scrupulously clean since every speck of dust causes disturbances in the light projected onto the dielectric.

The collimating lens is a plano-convex lens of 492mm focal length and 79mm diameter. The collimating lens also serves as the window into the vacuum chamber so it is mounted on an o-ring approximately 40mm from the optical flat.

The two surfaces which provide the multiple-beam interference are the lower metallised surface of an optical flat set in the upper electrode and the upper surface of the dielectric. The optical flat is a high quality quartz flat of 2 inch (50.8mm) diameter and 0.5 inch (12.7mm) thickness with a surface finish of $\lambda/20$. The flat was mounted on a 1mm bevel such that its lower metallised surface formed a continuous conducting plane with the flat portion of the electrode. The bevel of the optical flat was coated at the same time as the surface and hence provided a convenient conduction path between the optical flat and the electrode The incident beam was arranged so that it was a few degrees from normal allowing a prism to be used to direct the emerging beam onto a screen or towards a camera. Sometimes an image lens was used to adjust the size of the image.

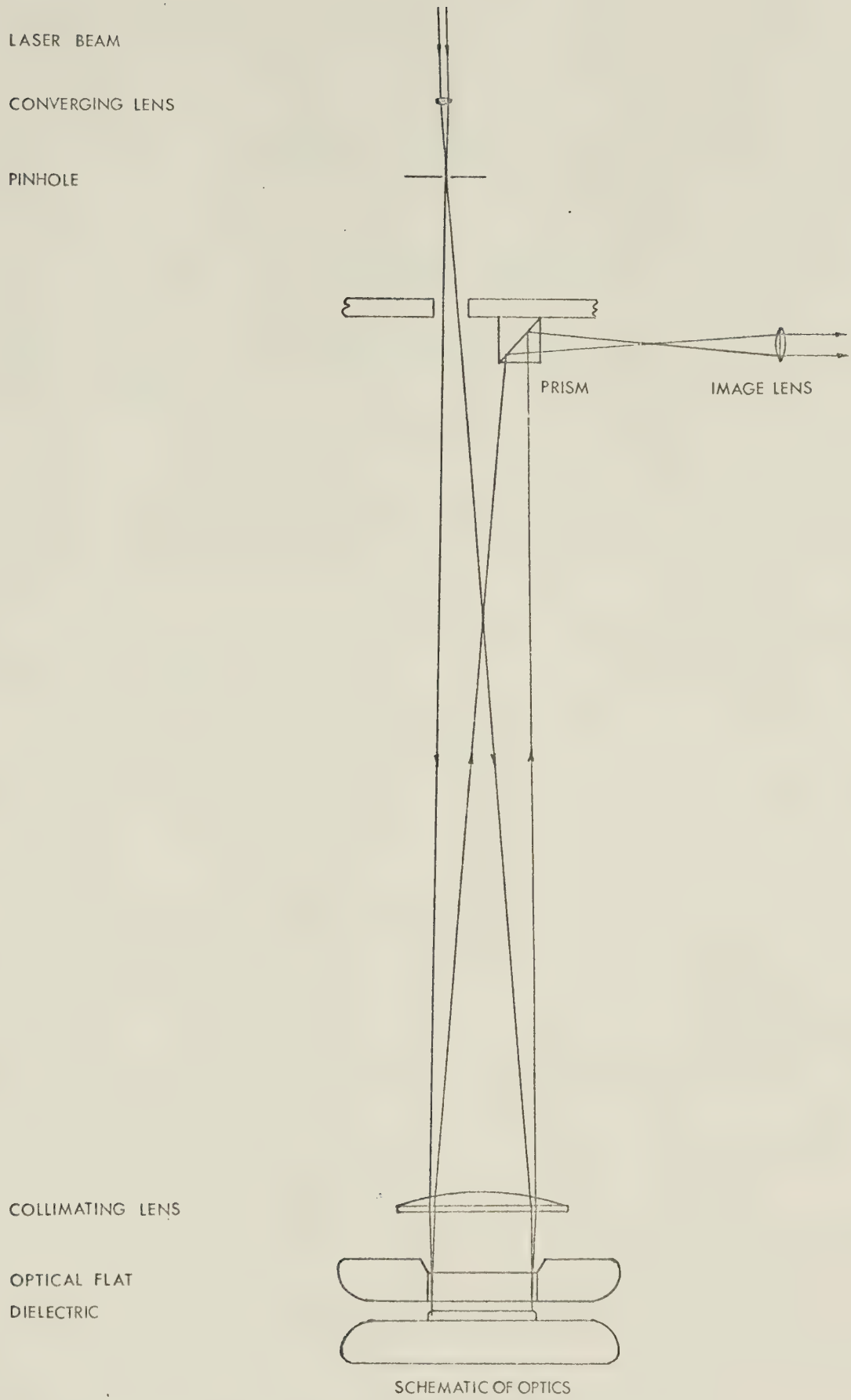
LASER BEAM
CONVERGING LENS
PINHOLE
PRISM
IMAGE LENS
COLLIMATING LENS
OPTICAL FLAT
DIELECTRIC
SCHEMATIC OF OPTICS

figure 8.1

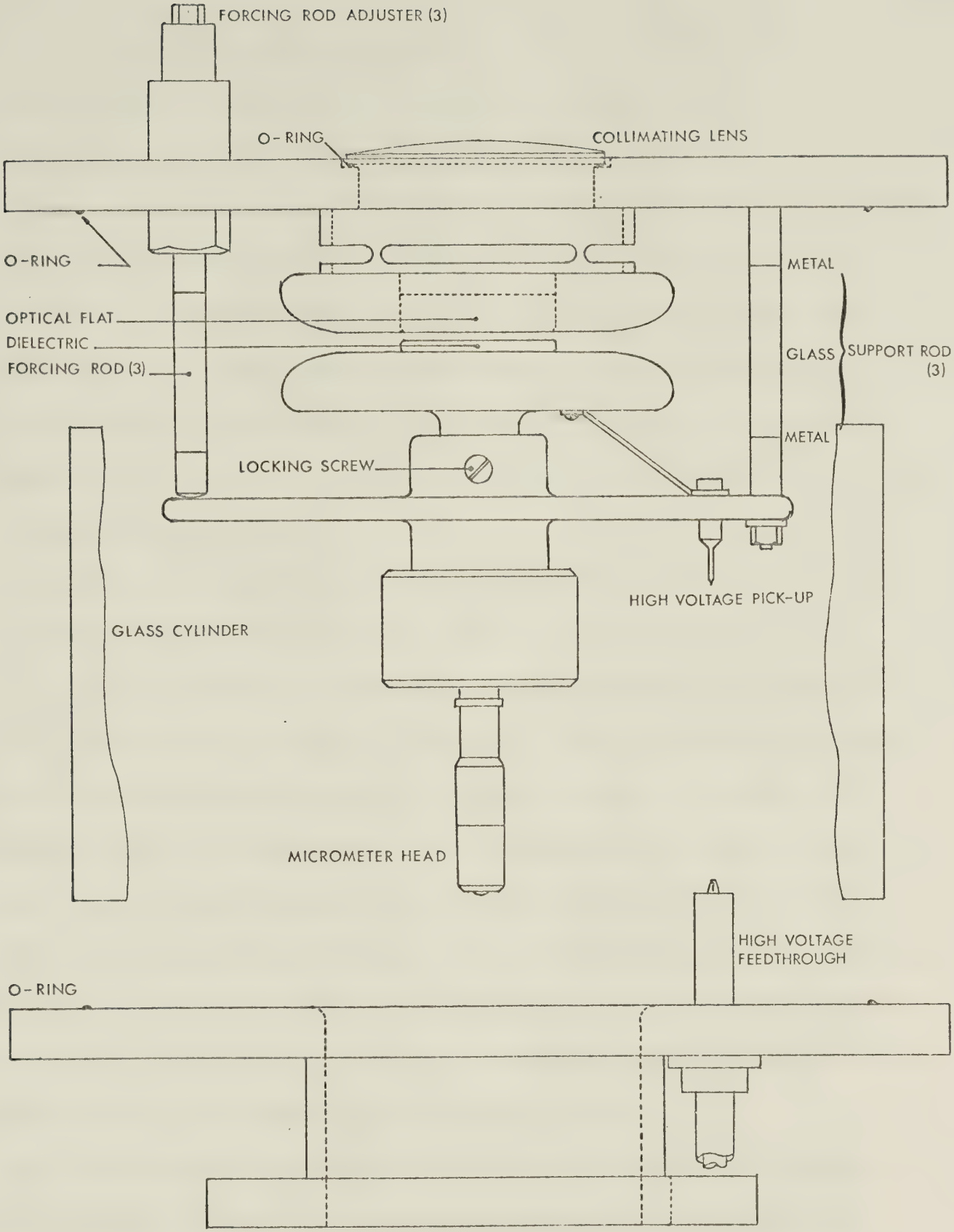
FORCING ROD ADJUSTER (3)
O-RING
COLLIMATING LENS
O-RING
METAL
OPTICAL FLAT
DIELECTRIC
FORCING ROD (3)
GLASS
SUPPORT ROD (3)
METAL
LOCKING SCREW
HIGH VOLTAGE PICK-UP
GLASS CYLINDER
MICROMETER HEAD
HIGH VOLTAGE FEEDTHROUGH
O-RING

figure 8.2

The two electrodes are supported as shown in figure 8.2. The upper electrode containing the optical flat is attached directly to the top plate. The lower electrode assembly is suspended from the top plate by three glass rods spaced 120° apart. The spacing of the two electrodes can be adjusted by means of a micrometer head which moves the lower electrode. The parallelism is adjusted by three glass forcing rods arranged on the same diameter as the support rods and interspersed between them. By being moved up and down by vacuum tight screw adjusters, these rods tilt the entire assembly allowing it to be brought to any position desired.

Since the electrode assembly is suspended entirely from insulators the whole assembly is floated at high voltage.

As the experiment proceeded it became necessary to modify the lower electrode. The original intention had been to provide a uniform field over the dielectric and by suitable rounding of the edges to avoid any field concentrations. This arrangement had worked in the experiment for measuring the forces where breakdown through the dielectric was sometimes obtained. In the present case,when the optical flat was used,breakdown invariably occurred around the edge of the dielectric. In an effort to produce breakdown on the flat surface of the dielectric the following measures were taken :

1) The dielectric was reduced from 5 cm diameter to 4 cm diameter. It was thought that if the edge of the dielectric were removed from being opposite the discontinuity at the edge of the optical flat the likelihood of edge breakdown would be reduced. The result was to cause breakdown straight across the gap from the dielectric edge to the optical flat.

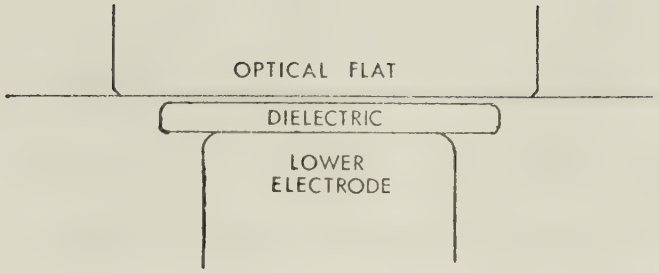

figure 8.3.

2) The lower electrode was replaced by one in the form of a right circular cylinder with rounded edges as shown in figure 8.3. Early experiments with this set-up gave currents of several hundred nanoamps due, it was thought, to the removal of the chromium coating on the corner of the optical flat between the face and the bevel which had become exposed due to repeated polishings of the upper electrode.

3) To cure the problem of the coating being removed, the outer part of the face and the bevel were coated with about a thousand angstroms of chromium leaving a central 4.5 cm diameter area for the interferometer.

8.2 Metallising the optical flat

As was seen in section 7.2, the sharpest fringes are obtained by using the highest reflectivity possible. In this case the reflectivities of the two surfaces are different so the factor $\sqrt{R_1 R_2}$ must be used. The reflection coefficient of polished titania is 0.18 therefore it is particularly important that the coefficient of the metal coating on the optical flat be as high as possible.

The first choice was aluminium which was the same material as the electrodes and had very good optical properties. Unfortunately the evaporated aluminium was pulled off by the electric field at voltages much lower than those encountered in the breakdown tests. Even a sputtered aluminium coating was pulled off at only 30 kv across

2.5mm or 120 kV/cm. Silver coatings were also tried with similar results. Chromium coatings showed great promise with their great adhesion to the substrate and a sample tested remained on the flat until it was damaged by the spark at breakdown of the vacuum gap. A coating of 150 Å thickness should have a reflectivity of 0.6[10] and an absorption of about 0.04[11]. These values are for evaporated films but because of the continuous structure of even the thinnest evaporated chromium films they should also be valid for sputtered films.

The films obtained had quite different properties and so a series of films were made on glass slides with the results shown in figure 8.4. The thickness of the films was calculated on the basis that a 300 second film was about 825 Å thick and that the thickness is directly proportional to the time.

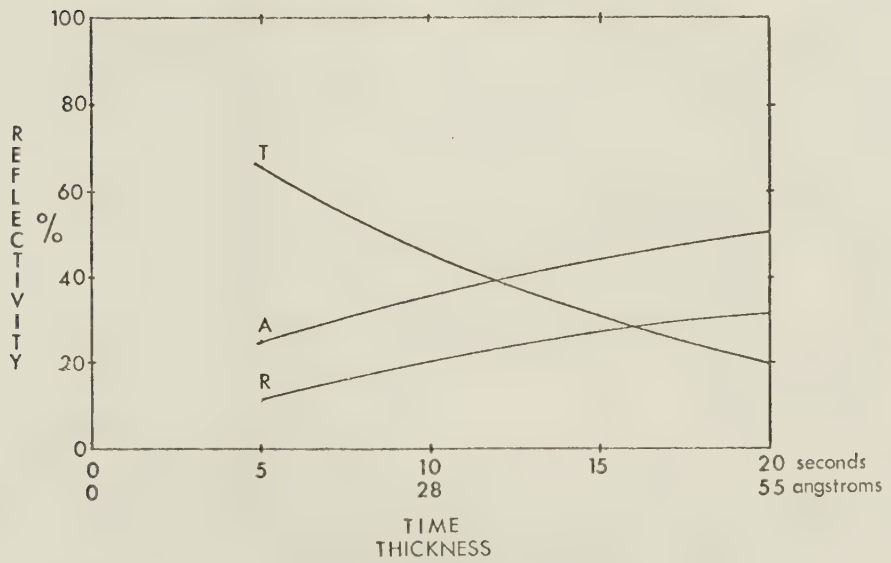

figure 8.4

These results were obtained on glass microscope slides which had been carefully cleaned and using Marz grade (99.99% pure) Chromium. Due to the low reflection and the high absorption obtained, an interferometer using such a coating would be basically only a two beam interferometer.

An alternative coating was investigated using a conducting tin oxide film based on the techniques described by Gomer[13] and Livesey, Lyford and Moore[14]. In this technique the glass to be coated was placed in an oven and brought to 450°C. Stannous chloride was heated in a glass tube outside the oven while oxygen was passed over it ; the resulting white fumes being carried into the oven and deposited on the glass. The most difficult aspect of this technique was making the film uniform. The final set up used was that shown in figure 8.5a with an outlet as shown in 8.5b. With this arrangement it was possible to produce a coating with a thickness between 0.75 μ and 0.85 μ over an area about 12 cm diameter. These coatings had a resistance of

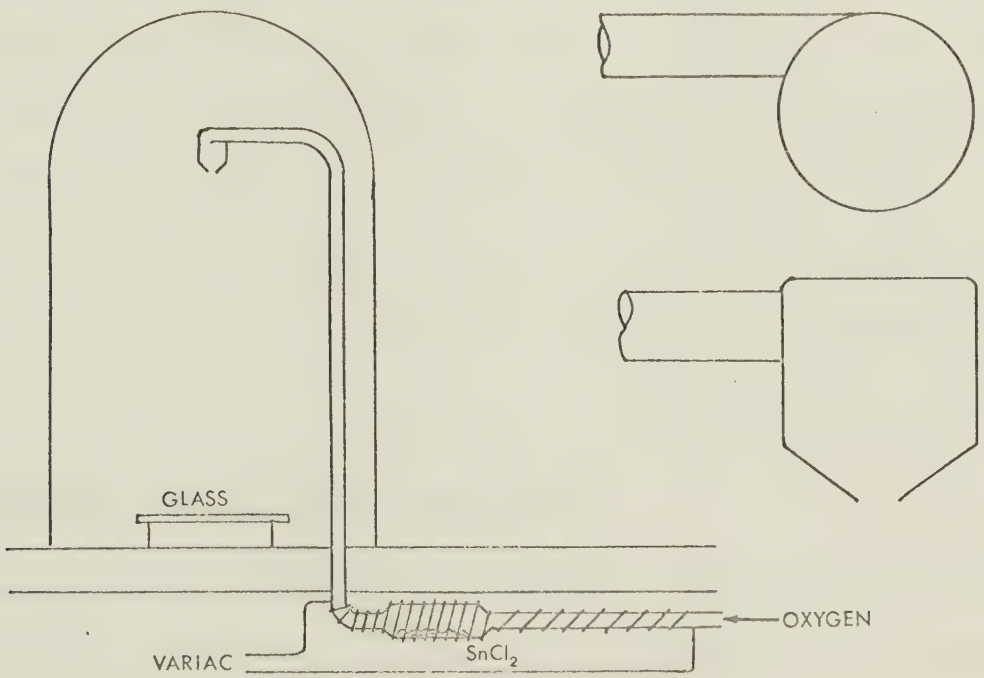

(a) (b)

figure 8.5

about 100Ω per square, equivalent to a resistivity of 10^{-2}Ωcm. Unfortunately coatings of this thickness exhibited a slight translucence or milkiness. The maximum reflectivity obtainable from a quarter wavelength coating would be 0.2.

Comparing coatings of the two materials with equal reflection coefficients, one sees that the stannic oxide has the advantages of lower resistivity and lower light absorption but the disadvantage of a less uniform, rougher surface. Since this experiment was intended to study effects arising from the surface inhomogeneities of a dielectric, it was thought that the chromium was a better material because it introduced fewer unknowns. Hence a 10 second (30 Å) chromium coating of 500Ω per square was used.

Using the value of 0.2 for the reflection coefficient of both surfaces and using equation 7.10, a value of 3 is determined for the finesse. Accepting Tolansky's[9] statement that determinations can be made to a tenth of a fringe width, an ultimate resolution of 100Å should be realized. While a perturbation of that size could be detected if it should be crossed by a fringe, it would remain undetected if it came between fringes. To ensure detection, any disturbance would have to equal the fringe spacing, approximately 3000Å.

8.3 Possible range of surface movements.

Having established the minimum motion detectable with the apparatus it is instructive to see what range of surface movements

may be expected from various dielectrics. Since one is looking for local effects of unknown magnitude it is difficult to get an accurate estimate of the surface distortion. However, it is possible to make an approximation to the overall motion which will at least give an order of magnitude estimate of the displacements involved.

Three possible causes of motion of the dielectric surface relative to the optical flat are : 1) mechanical expansion of the dielectric due to the force exerted by the field, 2) expansion due to heating of the dielectric by the currents flowing, 3) flexing of the lower electrode support structure.

Consider the dielectric as a very short thick rod under tension with one end glued to the lower electrode and the other being pulled by the electric field. Then

$$\frac{F}{A} = M_y \frac{e}{l_o} \qquad (8.1)$$

where 'F' is the force, 'A' is the area, 'e' the elongation, 'l_o' the initial length,'M_y' is Young's modulus which has the dimensions force/area. Consider a dielectric disc of diameter 5cm and 3mm thickness. If one has a force of 1Kg, which is quite possible from section 5.3, then (8.1) becomes on rearranging and substituting constants:

$$e = \frac{1.5}{M_y} \times 10^{-4} \text{ metres} \qquad (8.2)$$

M_y being in Kg/cm^2.

The following table gives Young's modulus and elongation for titania and a few other dielectrics.

Material	M_y (kg/cm^2)	Elongation (Å)
Titania	$1\text{-}1.5 \times 10^6$	1.5
Alumina	3.5×10^6	0.5
Plexiglass	4.5×10^4	35
Teflon	4.0×10^3	400
Phenolic (pure)	$2.5\text{-}9 \times 10^4$	<60

It would seem that there is little prospect of observing any deformation due to mechanical forces alone on either the surface of the titania or alumina. However, in practical cases the field distribution is not always uniform but rather there can be considerable local field enhancement as pointed out by Cranberg and Hawley.[12] A practical problem arises however in that the softer materials which show most elongation are the most difficult to polish. In addition materials such as plexiglass have a very low reflection coefficient which degrades the resolution of the interferometer. Since the titania discs were available and easily polished, it was decided to consider this case.

Consider the thermal expansion of a titania disc. The expansion is described by the relation :

$$e = \alpha l \Delta T \qquad (8.3)$$

For titania $\alpha = 8.3 \times 10^{-6}/°C$, and since '1' the length of the disc is 3mm,

then,

$$e = 250 \text{ Å}/°C \qquad (8.4)$$

Englefield et al.[4] report a temperature rise from 20°C to 300°C immediately prior to breakdown. Even at 20 kV, which in their case was 10 kV below breakdown the temperature had risen to 90°C, a rise of 70°C. This would be equal to an expansion of three wavelengths or six fringes. It can be seen that a local hot spot only 12°C warmer than its surroundings should cause a fringe to form. Thus it is seen that any surface movement observed will arise from the heating of the locality by the field concentration rather than by mechanical stretching of the material, although the two effects will reinforee one another.

The third possible cause of relative movement of the surface of the dielectric is that caused by flexing of the supporting structure. Rather than attempt to calculate this motion it was decided to measure it by loading the structure with a weight simulating the force due to the field and measuring the actual motion observed. The results of these tests are shown in figure 8.6.

In summary, the three sources of movement may be considered thus: any movement due to mechanical force on the dielectric will be too small to be observed; the flexing of the support structure will cause a bulk motion of the order of three fringes; nevertheless, any local expansion due to local heating of more than a few degrees should be observed.

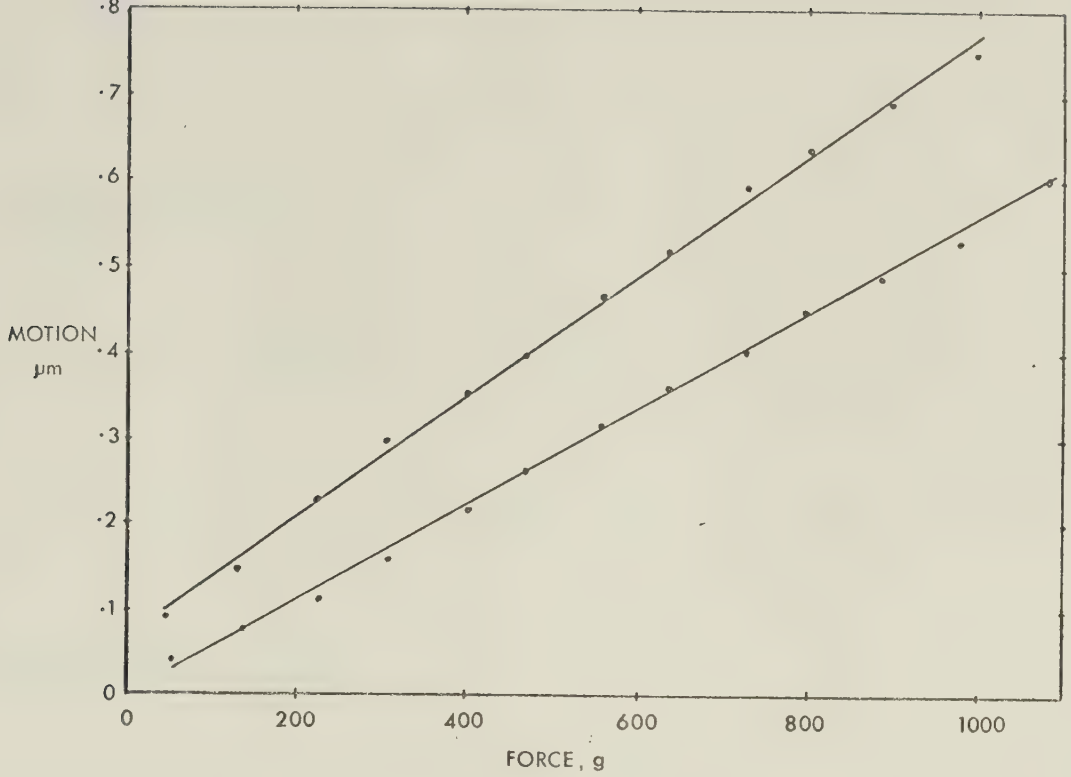

figure 8.6.

Tests were performed on a piece of titania to see if these conditions were attainable in practice. A piece of titania which had already been broken down was used since the breakdown path formed a convenient resistance of about a thousand ohms through which current could be passed to heat up a portion of the ceramic. These tests were carried out in the usual apparatus, the only difference being that they were done at atmospheric pressure. It was found that a power of approximately 100mW would produce detectable changes in the fringe pattern while greater power of about a watt would cause a new ring to form around the heated area. Since powers of about 100mW in the dielectric have been recorded[4] at as much as 6kV before breakdown, it was concluded that the technique should be a useful means of investigating the surface.

8.4 Vacuum equipment

The vacuum equipment was identical to that described in section 3.2 except that the apparatus was enclosed in a glass cylinder 10 inch diameter by 6 inch height. Due to a generally cleaner system the ultimate pressure was about 2×10^{-7} torr with a general working pressure of 5×10^{-7} torr.

8.5 Electrical equipment

The same high voltage set described in section 3.3. was used initially. In later experiments as a result of a failure in the H. V. set it was replaced with a Universal Voltronics model BAL-50-16, having maximum voltage and current ratings of 50 kV and 16 mA respectively. The current across the vacuum gap was measured using the circuit in figure 8.7.

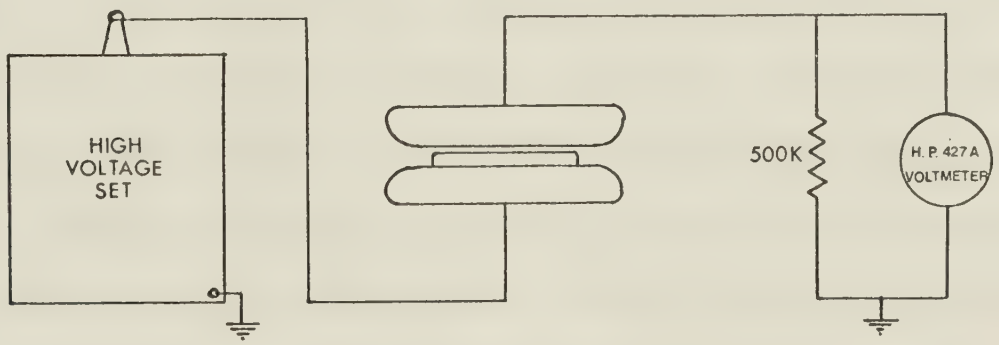

figure 8.7.

In early runs the 500 KΩ resistor - voltmeter was replaced by a pico-ammeter. The results of the two systems were identical and since the voltmeter was more readily available it was used for most of the experiments.

9. EXPERIMENTAL PROCEDURE

9.1 Adjusting for fringes.

The entire apparatus is assembled ex vacuo, the top plate being supported by three metal rods mounted on the base plate. The dielectric and the optical flat are brought together until they are almost touching. Next they are made approximately parallel using the adjusters and judging the parallelism of the two surfaces by eye. Then the laser is turned on and usually there will be a wedge of about twenty fringes visible. Using the screw adjusters the two surfaces are made parallel. Usually at this stage there will be a couple of rings due to the warping of the dielectric by the setting of the glue.

Once a good set of fringes has been obtained the two electrodes are gently brought together, then using the micrometer, the lower electrode is backed off to the desired spacing. Finally the lower electrode is locked in position to prevent any movement due to take up of slack in the threads when the field is applied. During the movement and locking of the electrode the fringe pattern does not remain static since it is impractical to build a device with sufficient precision. However, the pattern does not move very far and is easily identifiable, hence it only takes a few seconds to recover the pattern.

When the desired fringe pattern is achieved, the upper plate is lifted off the three metal rods which are then removed. The glass cylinder is put in their place and the upper plate lowered so that the o-rings are sitting on the cylinder while the high voltage pick-up is carefully inserted in the feedthrough at the same time.

The chamber is then pumped down and the experiment is ready to proceed as soon as the pressure is of the order of 10^{-6} torr.

9.2 Recording the fringes

All measurements were undertaken using a vacuum gap of 0.051cm. which should lead to breakdown between 24 kV and 28 kV on the basis of earlier tests.

Initially the voltage was raised to 10 kV and the fringe pattern projected on a screen so that it could be observed. As expected, the only change visible was a gradual overall movement as the force due to the electric field flexed the supporting structure. For higher voltages the outgoing beam from the interferometer was projected into a Beaulieu 16mm movie camera from which the lens had been removed so that the image was projected directly onto the film. Filming was done at 64 frames per second using Kodak Tri-X film. A 4x filter was inserted in the light path between the pinhole and the collimating lens reducing the light intensity by a factor of 16 since the light must pass through it twice.

The voltage was increased from 10 kV to about 22.7 kV in just under 60 seconds. The only effect visible on the film was a blurring of fringes at breakdown and a few blank frames due to the rapidity with which the fringes were moving. It was thought that this movement was due to the mechanical relaxation of the supporting structure when the field was suddenly removed. To test this hypothesis the experiment which had been done to determine the extent of motion of the supporting structure was repeated but this time the weights were suddenly removed, the whole procedure being filmed at 64 frames per second. The film showed similar behaviour to that seen at breakdown; so it was concluded that the cause of the motion had been identified.

This overall motion did not exclude the possibility of some local

motion which was being missed due to the blurring of the fringes. Hence it was decided to do the filming around breakdown at 500 fps using a Hycam rotating-prism type 16 mm high speed motion picture camera. Enough light was available for these higher speeds by merely removing the filter. In early tests it was noted that breakdown was occurring on the edges of the titania, suggesting that perhaps this breakdown was due to some field concentration between the edge of the dielectric and the possible discontinuity where the optical flat joined the electrode. For this reason the dielectric was reduced from 5 cm diameter to 4 cm so that the two edges were not opposite one another.

Thus the final procedure followed was as follows. First the voltage was increased a few kV at a time while monitoring the current flowing through the dielectric. Photographs of the fringe pattern were taken at intervals with a Graphlex camera. Once within a few kV of the expected breakdown voltage, the Hycam was started and the voltage rapidly (within 30 seconds) increased to breakdown.

10. RESULTS

10.1 Prebreakdown current

After a suitable film had been obtained on the optical flat, the apparatus was assembled and adjusted with a vacuum gap of 0.051 cm (0.020 in.). All measurements were taken at pressures of 10^{-6} torr or less. The voltage was raised to 20 kV for both the ceramic cathode and anode in steps of 2 kV per hour for voltages higher than 10 kV. In the first test, pictures were taken every quarter hour, but in later runs only immediately before and after a change of voltage. The only change in the fringe pattern was a gradual movement due to the electrodes being pulled together as explained in section 8.3.

Since no sign of any change in the fringes had been detected, it was decided to repeat the experiment while monitoring the current. The results are shown in figure 10.1

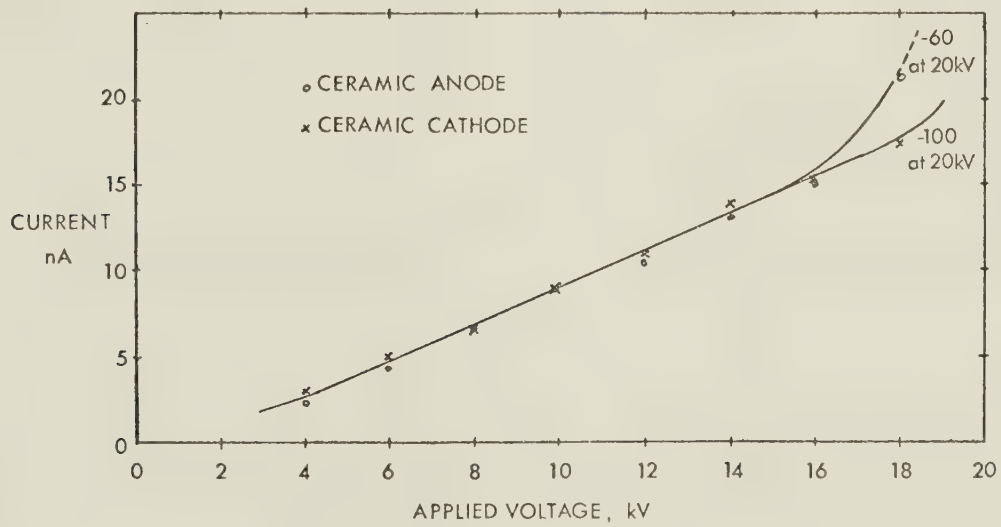

figure 10.1

Due to the low currents, it is not surprising that no effects were seen in the fringes. These readings showed rapid fluctuations of one to two nA, that is the meter reading was not steady but rather vibrated over that amplitude. Since the last readings in each case showed rapid

increases in current, it was thought that breakdown might still occur at about 24 kV as suggested by previous measurements and be presaged by a large enough current flow to cause disturbances in the fringes.

Consequently the Hycam was set up and the voltage brought to 19 kV and filming commenced. The voltage was raised to 25 kV over a period of 30 seconds allowed by the length of the film (400 ft.). There was no breakdown. A 100 ft. roll was put in the camera and the voltage increased to 35 kV over 10 seconds and still there was no breakdown. The filming was done in the ceramic anode configuration.

It was decided to measure the current up to the maximum voltage yet reached. The results are shown in figure 10.2.

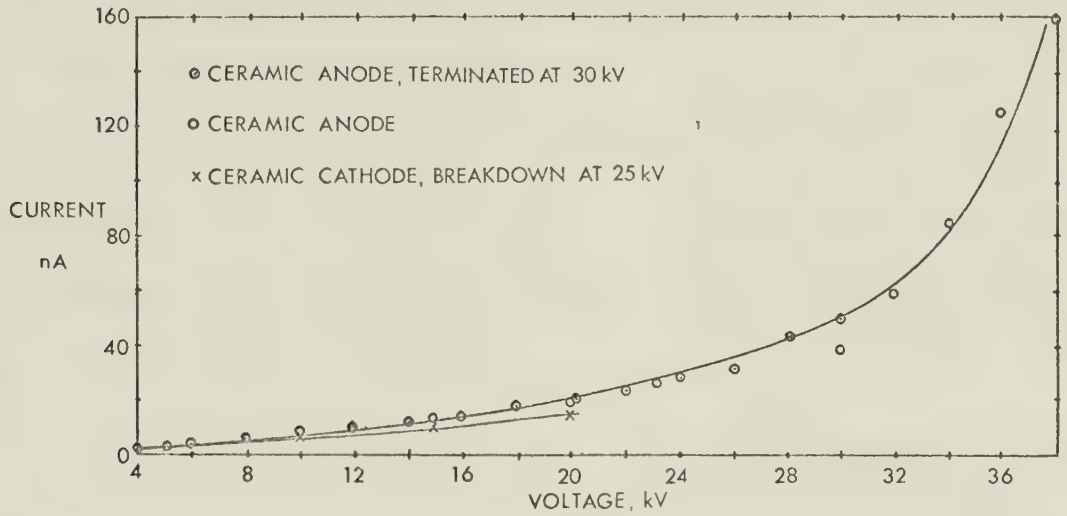

figure 10.2.

The first run was terminated at 30 kV due to failure of the high voltage supply. It will be noted that the currents are slightly lower than those previously recorded and that there is no increase in current at 20 kV, but a more gradual increase above 30 kV. Both these tests were for the ceramic anode case. For the ceramic cathode the same behaviour was found up to 20 kV but at 25 kV after a few minutes at about 20 nA the

current suddenly increased to 3.4 μA accompanied by a blue glow in the vacuum gap and an increase in pressure. The chromium coating was removed at the points of the glowing. The voltage was lowered while still measuring the current and at 20 kV the current was 2.2 μA indicating an impedance of about 10^{10} ohms.

Observation of the fringe pattern throughout all these measurements showed no surface distortions.

The chromium film was subsequently measured and found to have an impedance of about 10^{10} ohms. It had not been measured prior to use for fear of damaging it but other films had shown impedances in the order of thousands or hundreds of ohms. It must be concluded that the coating was not chromium but primarily impurities, a conclusion borne out by further study of the coating technique.

The results prior to breakdown should still be valid since the current (26 nA at 25 kV) indicates an impedance of 10^{12} ohms, and hence the voltage dropped across the film being about 1% is negligible. At breakdown the impedance of the gap would be zero and all the voltage would be across the film.

The experiment was repeated using more carefully controlled films which were checked for about 500 Ω per square prior to use, with the results shown in figure 10.3. It will be seen that the results are generally the same as with the impure film previously described. Also in figure 10.3 are shown the results of an experiment in which the optical flat was replaced with a disc of aluminium. There was no noticeable change in the pre-breakdown current. A breakdown very similar to that of figure 5.10 occurred as shown in figure 10.4.

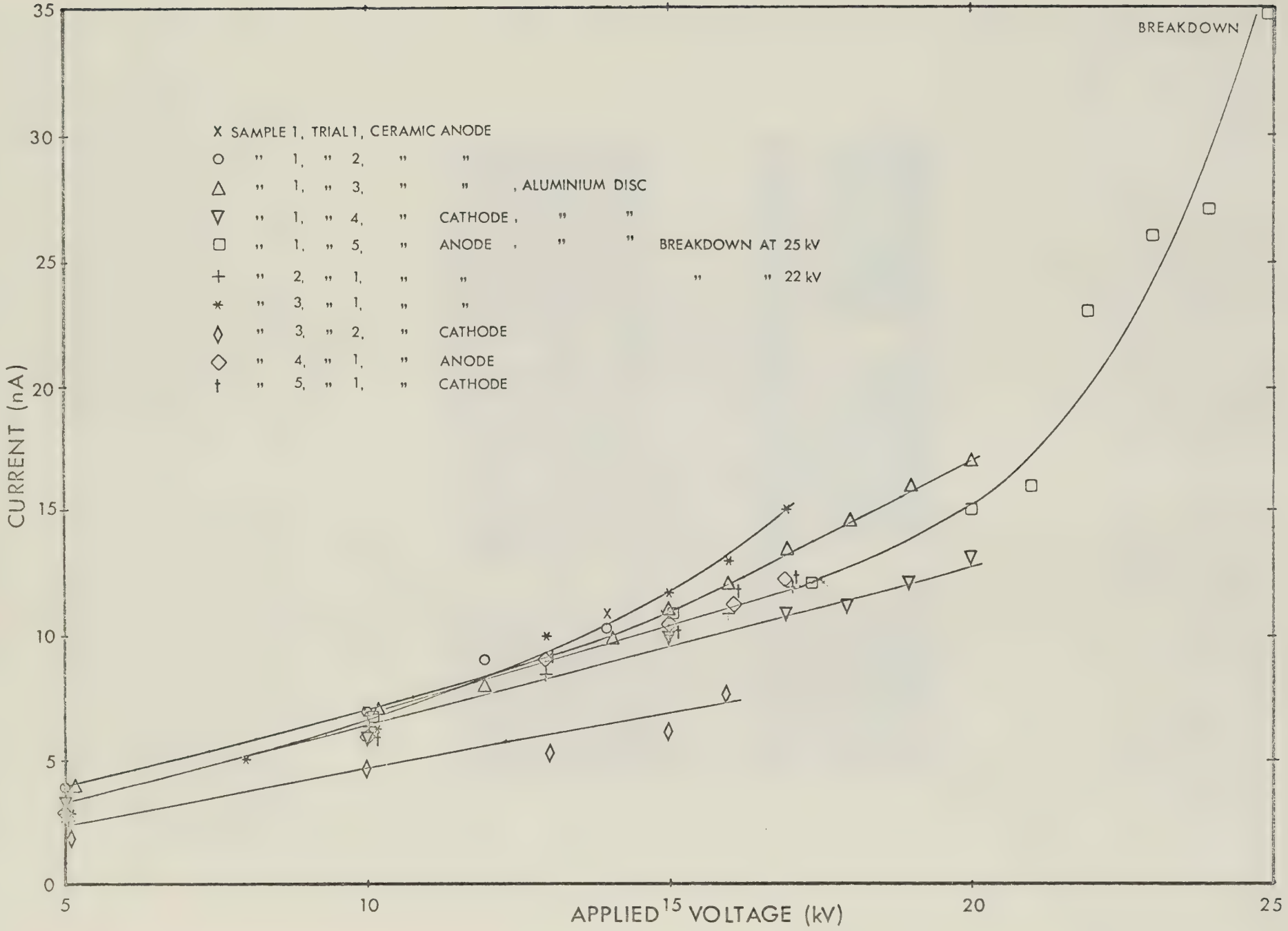
BREAKDOWN
X SAMPLE 1, TRIAL 1, CERAMIC ANODE
○ " 1, " 2, " "
△ " 1, " 3, " " , ALUMINIUM DISC
▽ " 1, " 4, " CATHODE , " "
□ " 1, " 5, " ANODE , " "
+ " 2, " 1, " "
* " 3, " 1, " "
◊ " 3, " 2, " CATHODE
◇ " 4, " 1, " ANODE
† " 5, " 1, " CATHODE
BREAKDOWN AT 25 kV
" " 22 kV
CURRENT (nA)
APPLIED VOLTAGE (kV)
0
5
10
15
20
25
30
35

figure 10.2

This illustration shows the breakdown path through the titania after the smaller part of the disc had fallen away. It can be seen that a piece of titania has been torn out of the surface and is bridging the vacuum gap.

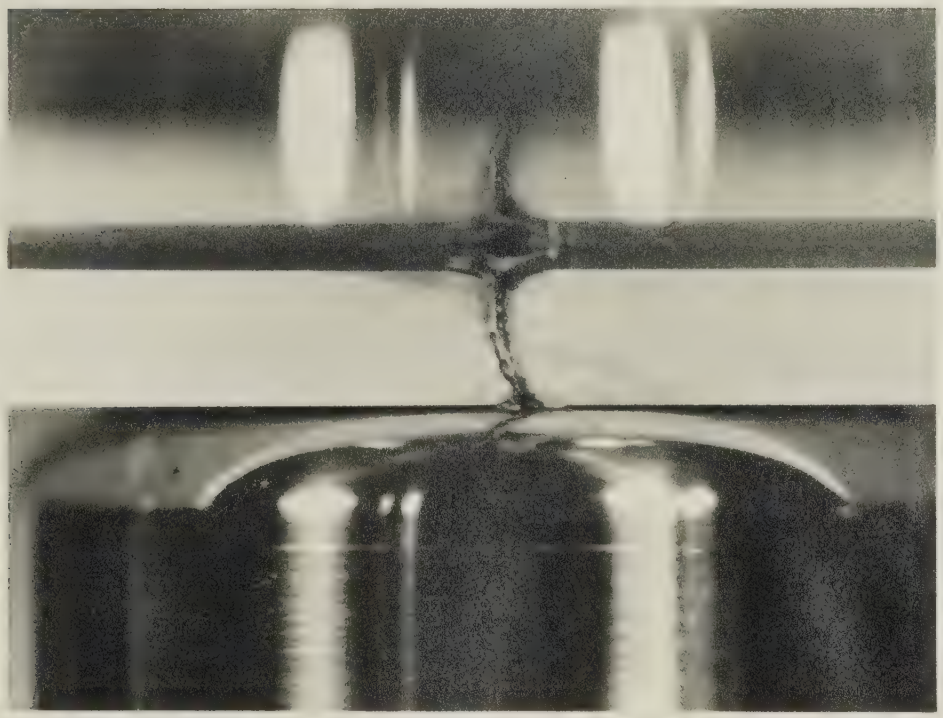

figure 10.4

In a further attempt to bring about breakdown within the field of view, the transparent area of the optical flat was reduced to 3.2 cm diameter so that a spark passing in a straight line from the rounded edge of the lower electrode to the edge of the thicker coating would have to pass through the dielectric in the area of observation.

10.2 Breakdown behaviour of the ceramic anode.

This experiment was carried out with the titania as the ceramic anode. This sample is labelled number 4 on figure 10.3. It can be seen that the currents obtained match those for the aluminium disc almost exactly. After being at 17 kV for an hour, the camera was started and the voltage increased. At about 22 kV, which was reached after approximately 15 seconds, there was sparking in the vacuum gap. This can be seen clearly in the film because of the wild motion of the fringe pattern about the surface. Enough current was not drawn to activate the trip-out mechanism of the high voltage supply which was set for 1 mA. The high voltage was further increased to between 25 and 26 kV when breakdown occurred. About 25 seconds elapsed between 17 kV and 26 kV. Ten frames from the film are shown in figure 10.5.

Figure 10.5.1, the last undisturbed frame, shows the pattern which had persisted throughout the film up to this point. This shows the surface of the titania as being convex by three fringes or about one micron.

Figure 10.5.2 shows the first signs of impending breakdown, three small patterns superimposed on the main pattern. They are typical of diffraction patterns around damage to the coating on the optical flat. The spot (a) appeared two milliseconds after figure 10.5.1, the other two spots appear for the first time on this frame taken at $t = 0.016$ sec.

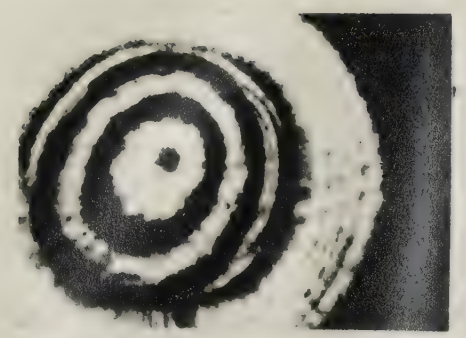

fig. 10.5.1 t = 0.000 sec.

fig. 10.5.2 t = 0.016 sec.

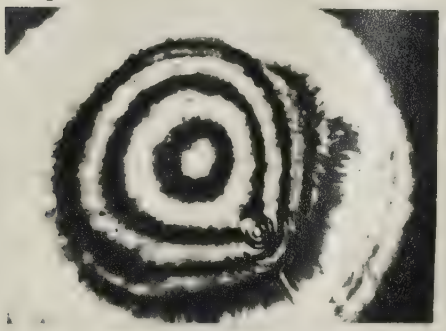

fig. 10.5.3 t = 0.074 sec.

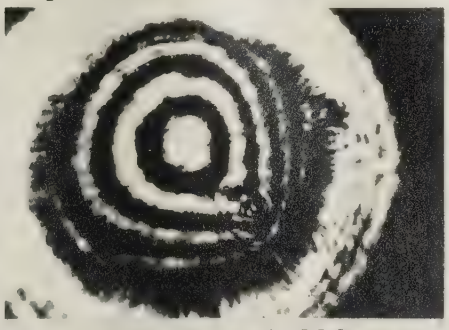

fig. 10.5.4 t = 0.118 sec.

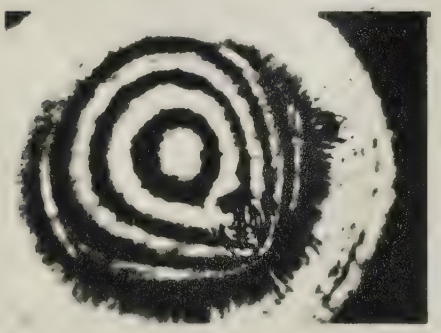

fig. 10.5.5 t = 0.154 sec.

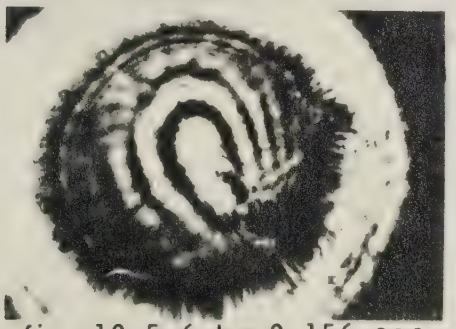

fig. 10.5.6 t = 0.156 sec.

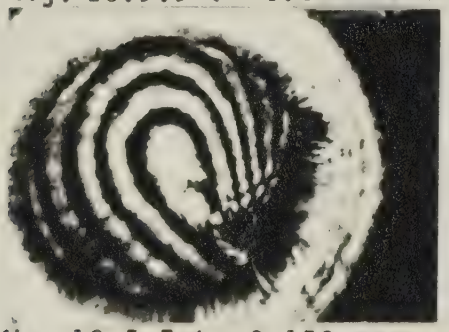

fig. 10.5.7 t = 0.158 sec.

fig. 10.5.8 t = 0.262 sec.

fig. 10.5.9 t = 0.836 sec.

fig. 10.5.10 t = 3.146 sec.

Figure 10.5.3, 10.5.4 and 10.5.5, taken at t = 0.074, 0.118 and 0.154 seconds respectively show the growth of the distortion around the spot (c). This development represents the expansion of the material about this area due to the heating from the current flow.

Figure 10.5.6, just 0.002 seconds after 10.5.5, shows a sudden change due to the cracking of the dielectric under thermal stress. This frame is blurred due to the rapid surface movement of the dielectric. Figure 10.5.7, the next frame, shows the same thing more clearly. This mechanical failure of the titania disc can indeed be considered the moment of final breakdown.

The subsequent frames, of which 10.5.8, 10.5.9 and 10.5.10 taken at t = 0.262, 0.836 and 3.146 seconds respectively are three examples, show a rapid flow of fringes with the collapse of the field. In the last frame the pattern is close to the original form apart from the disturbances due to the crack and the damaged coating.

On examination of the titania afterwards, there was a crack visible running from the edge through the spot (c) towards the centre. Also it was noted that a piece of titania around this spot had been torn loose and spattered on the optical flat thus accounting for the changed appearance of the spot (c) after breakdown.

In summary, the following phenomena have been observed. First a current flow is established between the surface of the dielectric and the optical flat. In a time of about 0.15 seconds the current flow sufficiently heats the titania to cause considerable local expansion.

This thermal shock causes the rupture of the titania during which a chip of titania is broken from the surface and pulled across the gap impinging on the opposite electrode. Following shut down of the high voltage supply the field collapses and the dielectric settles down to its modified shape, differing from the original only in the area of the crack.

10.3 Breakdown behaviour of ceramic cathode

The experiment was then repeated with the titania as the ceramic cathode. All the conditions were identical. Once again the high voltage was taken up to 17 kV while recording the current. As can be seen on figure 10.3, the results were identical. After an hour at 17 kV, the voltage was increased in roughly 15 seconds to about 24 kV at which point there was much flashing and sparking in the vacuum gap. The high voltage supply did not trip out meaning that the current had not exceeded 1 mA. The high voltage supply was turned off and the titania and coating examined for damage. Apart from some minor marks on the thicker part of the coating, no damage was visible. Consequently the high voltage was taken up to 22 kV at which point filming was started again. The voltage was rapidly increased until at about 27 kV breakdown occurred.

Ten frames from the film are seen in figure 10.6. Figure 10.6.1, which is the last undisturbed frame, shows the static pattern of the fringes. It can be seen that the area under observation has a large

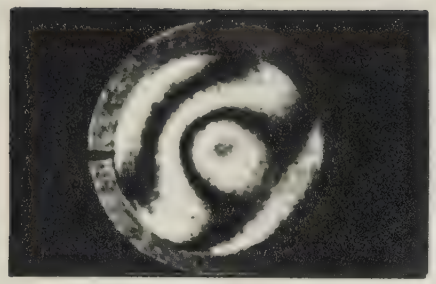

fig. 10.6.1 t = 0.000 sec.

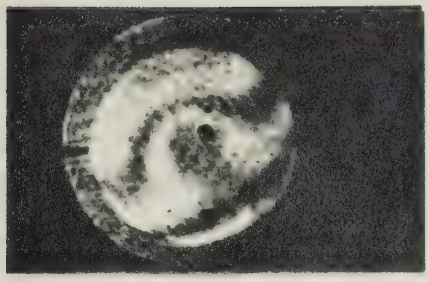

fig. 10.6.2 t = 0.008 sec.

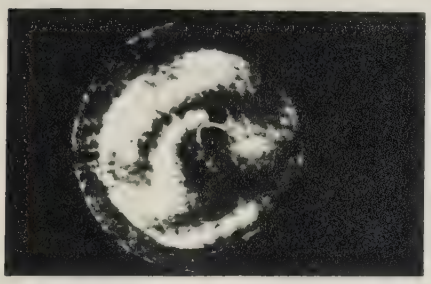

fig. 10.6.3 t = 0.044 sec.

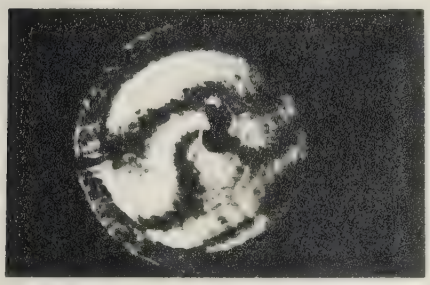

fig. 10.6.4 t = 0.060 sec.

fig. 10.6.5 t = 0.102 sec.

fig. 10.6.6. t = 0.208 sec.

fig. 10.6.7 t = 0.400 sec.

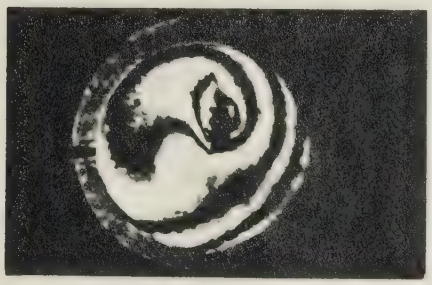

fig. 10.6.8 t = 0.700 sec.

fig. 10.6.9 t = 1.820 sec.

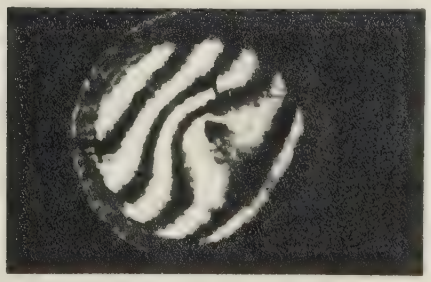

fig. 10.6.10 t = 5 minutes.

dimple slightly off centre. This frame is defined as being taken at t = 0.000 seconds.

Figure 10.6.2, taken at t = 0.008 seconds, shows a spot just off centre superimposed on a blurred pattern indicative of a rapidly moving surface. This spot grows very rapidly and is soon joined by another one as seen on figures 10.6.3 and 10.6.4 taken at t = 0.044 and 0.060 seconds respectively.

Two factors combine to complicate the interpretation of the frames of this film. First, the surface of the titania is initially quite complicated. Instead of a simple convex surface like the ceramic anode, the ceramic cathode has a slightly convex surface with a shallow circular depression. Second, the breakdown itself is not so clearly defined because this time there was no instantaneous event like the cracking of the dielectric.

Figure 10.6.5, taken at t = 0.102 seconds is probably just shortly after breakdown. After this frame, the fringes seem steadier, there is a gradual progression from one frame to the next and a complete absence of blurred frames typical of sparking during breakdown. Also the loops around the convex portion of the surface decrease in size; an occurrence consistent with the spreading apart of the two interferometer plates as the field collapses.

As the film proceeds through figures 10.6.6, 10.6.7, 10.6.8 and 10.6.9, taken at t = 0.208, 0.400, 0.700 and 1.820 seconds respectively, the most noticeable feature is the resolution of the spot from a grey

mass into a group of distinct fringes. Perhaps this spot has only appeared as a fuzzy mass because the fringes were so close that any vibration or surface movement would blurr them all together. It is just possible that these areas have marked the growth of two very steep pinnacles which have arisen under the heating and stress of the high electric field in the early stages of breakdown. Subsequently these pinnacles subside and broaden as the electric field collapses.

Figure 10.6.10 was taken some minutes after breakdown and represents the surface after all distortions have subsided. This fringe pattern described a surface which is basically the same as that in figure 10.6.1, the difference between the two frames being caused by the tilting of the dielectric with respect to the optical flat.

On examination of the optical flat and the titania, marks were found corresponding to the two spots seen on the film. The titania at these points had been reduced and fragments of this titania were spattered on the optical flat. In addition the coating on the optical flat was criss-crossed with lines indicating where the chromium had been completely removed. This was the first time this effect was observed. Photographs of these surfaces are shown in figure 10.7.

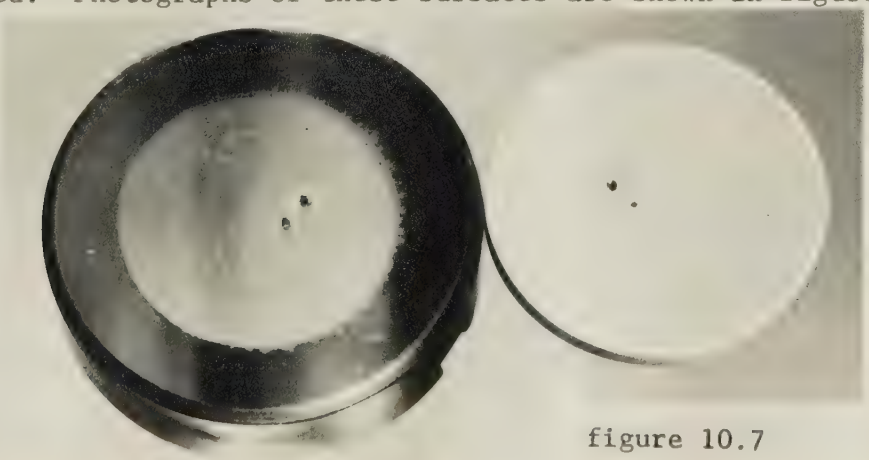

figure 10.7

11 CONCLUSIONS

An examination of the results in section 6 shows a general confirmation of Toso's results in that as the voltage increases above about 10 kV, an increasing fraction of the voltage is dropped across the titania. There is, however, some difference in the detailed behaviour. The differences in breakdown voltage may be attributed to the different geometry and to the use of samples of different area. Denholm [15] shows that for the difference between the sizes of the samples, the small one used by Toso would give a breakdown voltage some 25% higher than those used in the present work.

If the reduction of the titania due to resistive heating is the cause of breakdown, then clearly the breakdown is dependent on the energy absorbed by the dielectric. Thus the breakdown would be dependent not only on the voltage applied and the resulting current but also on the time during which it was applied. The measured currents were much lower than expected. The amount of power dissipated in the titania by these currents would be insufficient either to raise the bulk temperature of the titania or to cause any visible disturbance in the fringe pattern. The pre-breakdown currents decrease slightly with each cycling.

The main difference between the present experiments and previous ones is the form of titania used. Previous experiments used titania with ground surfaces, whereas in the present case the surfaces of the titania were optically flat. This change would have two principal

effects: first, the ground material would have a rougher surface possibly causing local field concentrations; second, the ground surface would have a larger surface area and hence contain more absorbed gas. Some combination of these two factors could account for the different results between present and past experiments.

Something of the breakdown mechanism has been revealed by the photography of the fringes. The first stage consists of a large current flow lasting between one and two tenths of a second. The passage of this current through the dielectric heats it up. This heating is visible in the expansion of the material which may be over an area of several square millimeters. The stress, or thermal shock, caused by this expansion may be sufficient to crack the dielectric. In most cases the breakdown is accompanied by the ejection of a small chip of titania from the breakdown spot which traverses the vacuum gap and impinges upon the opposite electrode.

Because only one sample was successfully tested at each polarity, it cannot be concluded whether the detail differences in the results were due to the individual samples or to the polarities.

It is suggested that breakdown occurs first across the vacuum gap, the prebreakdown current being supported by the outgassing of the titania. In support of this suggestion it should be noted that the breakdown stress of the vacuum gap is more nearly reproducible than that across the titania, as mentioned in section 6. In addition it has been observed that the prebreakdown current decreases slightly

each time a particular sample is tested. Also the fact that the prebreakdown current is slightly less after a sample has been pumped for a long time, suggests that the current is being supported by something which may be removed from the surface. In view of the porous nature of the sintered titania used for these experiments, absorbed gas would be a likely agent.

These experiments have established the practicality of the technique, nevertheless several refinements should be possible. The development of improved coatings would allow fringes of greater finesse allowing both higher resolution and the ability to sort out closely packed fringes. Different geometries may prove advantageous. Also it would be useful to monitor the current and voltage during breakdown. If these were displayed on an oscilloscope, an attachment for the Hycam would allow them to be recorded on the film simultaneously.

Since this technique is applicable to any dielectric, an investigation of other materials should prove rewarding. If suitable polishing techniques can be developed, softer materials should allow the examination of earlier stages in the breakdown mechanism. Another possibility would be to sputter a coating of titania or some other hard material on a softer base.

By various combinations of these refinements it should be possible to extend this technique to cover more of the breakdown mechanism in greater detail.

BIBLIOGRAPHY

1. Walker, G.B. and Lewis, E.L., Nature, Vol. 181, p. 38, (1958).

2. Hayes, R., Report M.L.4, Electrical Engineering, U.B.C., (1961).

3. Toso, L.W., M.Sc. Thesis, University of Alberta, (1965).

4. Englefield, C.G., Harwood, V.J., and Toso, L.W., I.E.E.E. Trans Elect Dev., Vol. ED-14, p. 443, (1967).

5. Bruce, F.M., Proc. I.E.E., Part II, Vol. 94, p. 138, (1947).

6. Kilpatrick, W.D., Rev. Sci. Instr., Vol. 28, p. 824, (1957).

7. Born, M. and Wolf, E., Principles of Optics, Pergamon, (1965).

8. Tolansky, S., An Introduction to Interferometry, Longmans Green and Co., (1955).

9. Tolansky, S., Multiple Beam Interferometry, Oxford, (1948).

10. Hass, G. and Ritter, E., Jour. of Vac. Sci. and Tech., Vol. 4, p. 71, (1966).

11. Sennett, R.S. and Scott, G.D., Jour. Opt. Soc. of Amer., Vol. 40, p. 203, (1950).

12. Cranberg, L. and Hawley, R., Research, Vol. 15, p. 347, (1962).

13. Gomer, R., Rev. Sci. Instr., Vol. 24, p. 993, (1953).

14. Livesey, R.G., Lyford, E. and Moore, H., Jour. of Sci. Instr. (Jour. of Physics E) Series 2, Vol. 1, p. 947, (1968).

15. Denholm, A.S., McCoy, F.J., and Coenraads, C.N., Proc. Symp. on Electrostatic Energy Conversion, PIC-ELE 209/1 (1963).